Journal Review: Separations: Materials, Devices and Processes

Extractive Distillation with Ionic Liquids: A Review

Zhigang Lei, Chengna Dai, Jiqin Zhu, and Biaohua Chen
State Key Laboratory of Chemical Resource Engineering, Beijing University of Chemical Technology, Box 266, Beijing 100029, China

DOI 10.1002/aic.14537
Published online July 2, 2014 in Wiley Online Library (wileyonlinelibrary.com)

Extractive distillation is commonly used for the separation of azeotropic or close-boiling mixtures in the chemical industry. During the past decade, the use of ionic liquids (ILs) as entrainers has received considerable attention due to their unique advantages when applied in extractive distillation. This work is devoted to providing an easy-to-read and comprehensive review on the recent progress made by chemical engineers, focusing on the issues of predictive thermodynamic models, structure-property relations, separation mechanisms, and process simulation and optimization. This review spans from the molecular level to the industrial scale, to provide a theoretical insight into the molecular interactions between ILs and the components to be separated. Moreover, a comprehensive database on the vapor–liquid equilibria and activity coefficients at infinite dilution concerning ILs is provided as Supporting Information. Concluding remarks are made on the unsolved scientific issues with respect to this promising special distillation technology. © 2014 American Institute of Chemical Engineers *AIChE J*, 60: 3312–3329, 2014

Keywords: extractive distillation, ionic liquids, predictive thermodynamic models, structure-property relations, separation mechanism, process simulation and optimization, review

Introduction

Extractive distillation is the most commonly used method for the separation of azeotropic or close-boiling mixtures in which an additional solvent (namely entrainer or separating agent) with a high boiling point is added to enhance the relative volatility of the components to be separated. In comparison with azeotropic distillation, where both the entrainer and components are heated to evaporate, extractive distillation saves energy because the entrainer does not need to be evaporated. In extractive distillation, the selection of a suitable entrainer is crucial to ensure an effective and economical separation process.[1–6] For a given homogenous mixture with key components i and j, the separation factor (i.e., selectivity) and capacity at infinite dilution are two important parameters for assessing various entrainers and are defined as[7,8]

$$S_{ij}^{\infty} = \gamma_i^{\infty} / \gamma_j^{\infty} \tag{1}$$

$$k_i^{\infty} = 1/\gamma_i^{\infty} \tag{2}$$

where γ_i^{∞} is the activity coefficient of component i at infinite dilution. Some ionic liquids ILs have a higher selectivity than common organic solvents; however, several ILs are not completely miscible over the full composition range with the components to be separated. A low capacity can lead to the liquid-liquid phase demixing and a second liquid phase being formed in the extractive distillation process. Thus, the dimensionless capacity k_i^{∞} defined by Eq. 2 is also an important physical quantity for evaluating the separation performance of different entrainers. A component with a small activity coefficient, which is a measure of solute and solvent interactions, will have a large capacity.[9]

There are five types of entrainers used in extractive distillation, that is, liquid solvents, solid salts (or dissolved salts), a mixture of liquid solvents and solid salts, hyperbranched polymers, and ILs.[10–19] The use of solid salts to obtain anhydrous alcohols dates back to the patents by Adolf Gorhan, which were the basis for the HIAG process.[20,21] Solid salts (e.g., $CaCl_2$, KAc, NaAc, and NaCl) are good entrainers when added into the reflux of an extractive distillation column (EDC).[22–24] Conversely, liquid solvents are easily entrained into the top product of the distillation column due to their volatility, whereas solid salts may erode the tray or packings, and the dissolution, reuse, and transport of solid salts are significant issues in industrial operation. For this reason, salt-containing extractive distillation technology using mixtures of solvents and salts as entrainers was developed in which the solid salt is first dissolved in the organic solvent and then added into the EDC.[25–27] Recently, the use of hyperbranched polymers and ILs has utilized the advantages of both solid salts (high separation ability) and liquid solvents (easy operation). However, studies on extractive distillation with hyperbranched polymers are rarely reported,[16–19] possibly due to the high price of hyperbranched polymers and the difficulty of finding chemical sources for general chemical engineers. ILs are a new class of solvents that are typically composed of a large organic cation and a small inorganic polyatomic anion, allowing them to exist in the liquid state around room temperature. Other advantages associated with

Additional Supporting Information may be found in the online version of this article.

Correspondence concerning this article should be addressed to Z. Lei at leizhg@mail.buct.edu.cn.

the use of ILs for extractive distillation are as follows: (1) no trace amount of ILs appearing in the distillate due to their negligible vapor pressure; (2) good solvent capacity for polar and nonpolar components to be separated; (3) fine-tuning of the physical properties by judicious combination of cations and anions, making them "designer solvents"; (4) high thermal and chemical stability and less corrosiveness; and (5) low melting points, which means that the IL-based devices can perform well at the low temperatures encountered in some chilled environments. In 2001, Arlt et al.[28,29] proposed the use of ILs as the entrainers for the separation of azeotropic or close-boiling mixtures with extractive distillation in their patents. In 2003, our research group first reported the separation of cyclohexane and toluene with $[BMIM]^+[AlCl_4]^-$, $[BMIM]^+[BF_4]^-$, and $[BMIM]^+[PF_6]^-$ as the entrainers of extractive distillation in a review article entitled "Extractive Distillation: A Review."[10] Since then, the number of studies relevant to extractive distillation with ILs has been growing dramatically, as seen from the Dortmund Data Bank on ionic liquid initiated by Prof. Dr. J. Gmehling, who collected a large amount of experimental data for 926 ILs, including activity coefficients at infinite dilution, liquid-liquid equilibrium (LLE), and vapor–liquid equilibrium (VLE) of binary and ternary systems.[30]

This is the first review devoted to providing an easy-to-read and comprehensive comment on extractive distillation with ILs. The impetus for doing so is threefold. First, during the past decade, an increasing number of ILs with different types of cations and anions has been synthesized in the laboratory, and their separation performance has been tested individually but not systemically. Therefore, it is necessary to identify the general relationship between the molecular structures of ILs and separation performance (e.g., selectivity and solvent capacity) by the combination of predictive thermodynamic models and experimental data measured by different research groups. Second, Meindersma et al.[31] reported that a pilot plant has been established for the separation of ethanol and water by extractive distillation with ILs. This is a significant improvement for the traditional process using the benchmark solvent ethylene glycol (EG) as entrainer,[32,33] with the result that energy consumption decreased by 16% after rational heat integration. Nowadays, many common ILs can be easily bought from chemical suppliers on a large scale and at low prices, rendering the application of this promising technology feasible in industry. Third, we would like to note the unsolved scientific issues from the viewpoint of chemical separation engineering by reviewing the recent publications to promote future development in this exciting field.

The rest of this review is arranged in a series of predictive thermodynamic models, structure-property relations, separation mechanisms, process simulation and optimization, and concluding remarks step by step. We first introduce the predictive thermodynamic models developed especially for systems containing ILs in the past decade, which are confined to group contribution methods (GCMs) and conductor-like screening model for real solvents (COSMO-RS) because their common characteristics are that the only input required is the molecular structures of the ILs and the components to be separated, and they have already been applied to (or can be readily extended to) the selection of ILs in extractive distillation. Although the classical local composition models, such as the nonrandom two-liquid equation and universal quasichemical theory of liquid mixtures (UNIQUAC) models, have also been successfully used for correlating the VLE experimental data for the systems containing ILs, they have no strong extrapolation power among systems. Then, the structure-property relations for the separation of nonpolar-nonpolar, polar–polar, and polar-nonpolar systems are summarized. In this regard, predictive thermodynamic models are indispensable due to the numerous combinations of cations and anions.[34] Afterward, the separation mechanism at the molecular level is clarified to provide a theoretical insight into the interactions between ILs and the components to be separated. At the macroscopic level, the extractive distillation process simulation and optimization are discussed, as well as the comparison of energy consumption among different special distillation technologies. Finally, some concluding remarks are presented. It is beyond our scope to review the synthesis of the specified ILs, and the meanings of abbreviations for anions and cations of all ILs throughout this review are given in Table S1 in the Supporting Information. The experimental activity coefficients at infinite dilution in ILs, which were exhaustively collected from the literature by the end of November 2013, are provided in Table S2 in the Supporting Information as a spreadsheet file that allows any reader to use conveniently.

Predictive Thermodynamic Models

UNIFAC-based models

Original UNIFAC Model. The original universal quasichemical functional-group activity coefficients (UNIFAC) model was proposed by Fredenslund et al. in 1975 based on an extension of the UNIQUAC model.[35] The activity coefficient of component i in the solution is calculated as the sum of two terms

$$\ln \gamma_i = \ln \gamma_i^C + \ln \gamma_i^R \tag{3}$$

where γ_i^C represents the combinatorial contribution to the activity coefficient essentially due to differences in the size and shape of the molecules, and γ_i^R represents the residual contribution to the activity coefficient essentially due to energetic interactions.

The combinatorial term is a function of two group parameters R_k and Q_k, which can be derived from references or calculated by $R_k = \frac{V_k \times N_A}{V_{VW}}$, $Q_k = \frac{A_k \times N_A}{A_{VW}}$, with V_{VW} of 15.17 $cm^3\ mol^{-1}$ and A_{VW} of 2.5×10^9 $cm^2\ mol^{-1}$, as suggested by Bondi.[36] A rapid and powerful approach to calculating the group volume R_k and surface area Q_k is through the use of the COSMO-RS model, and no experimental data are needed, which saves lots of labor and capital consumption. The application of the COSMO-RS model is no longer limited to predicting the thermodynamic properties of systems containing ILs. The residual term of the original UNIFAC model is a function of the group interaction parameters α_{nm} and α_{mn}. The detailed description can be found in the open literature.[37,38]

For the UNIFAC-based model, the most important work is the determination of the group binary interaction parameters α_{nm} and α_{mn} by fitting the experimental activity coefficients at infinite dilution and VLE or the liquid-liquid equilibria (LLE) data at finite concentration. Several versions of the original UNIFAC model for ILs, which are distinct from one another in the decomposition of the IL groups and the database used to fit the group binary interaction parameters, are listed in Supporting Information Table S2.[37–62] Alevizou

et al.[44] revealed that the group binary interaction parameters obtained by fitting the experimental activity coefficients at infinite dilution and LLE can be extended to describe the VLE very well. That is, the original UNIFAC models listed in Supporting Information Table S2 are applicable for guiding the entrainer screening and the VLE prediction with respect to ILs. However, the original UNIFAC model for ILs, as reported by Lei et al.,[37,38] is the most complete by far, including many more IL groups, and has, thus, been widely used for computer-aided molecular design (CAMD) of ILs and VLE prediction by many authors. Recently, the original UNIFAC model was further extended to describe IL-gas systems and has become a universal and reliable predictive thermodynamic model.[40]

Modified UNIFAC Model. The activity coefficient is also calculated by a sum of the combinatorial term and residual term. However, the combinatorial term is slightly changed in an empirical way and is written as

$$\ln \gamma_i^C = 1 - V_i' + \ln V_i' - 5q_i\left(1 - \frac{V_i}{F_i} + \ln\left(\frac{V_i}{F_i}\right)\right) \tag{4}$$

$$V_i' = \frac{r_i^{3/4}}{\sum_j x_j r_j^{3/4}}, V_i = \frac{r_i x_i}{\sum_j x_j r_j} \tag{5}$$

$$r_i = \sum v_k^{(i)} R_k, F_i = \frac{q_i x_i}{\sum_j x_j q_j}, q_i = \sum v_k^{(i)} Q_k \tag{6}$$

The residual term can be obtained using the following relations

$$\ln \gamma_i^R = \sum_k v_k^{(i)} (\ln \Gamma_k - \ln \Gamma_k^{(i)}) \tag{7}$$

$$\ln \Gamma_k = Q_k\left(1 - \ln\left(\sum_m \theta_m \psi_{mk}\right) - \sum_m \frac{\theta_m \psi_{km}}{\sum_n \theta_n \psi_{nm}}\right) \tag{8}$$

where the group area fraction θ_m and the group mole fraction X_m remain the same as in the original UNIFAC model. For a better description of the activity coefficients, a significant modification of introducing more group binary interaction parameters into the group interaction term is made and is expressed as

$$\psi_{nm} = \exp\left(-\frac{a_{nm} + b_{nm}T + c_{nm}T^2}{T}\right) \tag{9}$$

where a_{nm}, b_{nm}, and c_{nm} are the adjustable parameters in the modified UNIFAC model and should, thus, be determined beforehand.

The modified UNIFAC model for ILs was first proposed by Gmehling's research group due to its good prediction accuarcy.[45–57] However, only a limited number of IL groups are present in this model (see Supporting Information Table S2). Although the modified UNIFAC model can give better predictions, there are many model parameters to be determined from the experimental data. This means that if the database volume for some systems is not large enough, the group binary interaction parameters to be regressed are sensitive to the initial values arbitrarily given during the regression procedure. In this case, the calculation for these systems exhibits a correlative rather than a predictive character.

The UNIFAC-based models are familiar to general chemical engineers because their model equations are simple and can be directly incorporated into the current process simulation software, such as ASPEN PLUS, PROII, and ChemCAD, among others, for process simulation and optimization. Therefore, more efforts should be made to expand the database volume to fill the gaps remaining in the current parameter matrix of the UNIFAC-based models.

ASOG models

Like the UNIFAC-based models, in analytical solution of groups (ASOG) models, the activity coefficient of component i in the solution is also calculated as the sum of two terms[58,59]

$$\ln \gamma_i = \ln \gamma_i^{FH} + \ln \gamma_i^{G} \tag{10}$$

where the superscripts "FH" and "G" represent a "Flory–Huggins" combinatorial contribution and a "group" residual contribution to the activity coefficient, respectively.

Inoue et al.[60] first extended the ASOG model to systems containing ILs, correlating the activity coefficients at infinite dilution of *n*-alkanes in $[BMIM]^+[BF_4]^-$. Later, Robles et al.[61,62] predicted the LLE for binary and ternary systems containing ILs using the ASOG model, leading to a satisfactory result. The cations involved are limited to imidazolium (IM) and pyridinium (PY), and the anions are tetrafluoroborate (BF_4) and hexafluorophosphate (PF_6). With the same group interaction parameters, the ASOG model has the potential to predict the VLE of systems containing ILs. Unfortunately, the current studies on the ASOG model are still limited.

COSMO-RS models

Model Description. The COSMO-RS model, first proposed by Klamt and coworkers,[63–69] is an *a priori* predictive model that only requires information on the atoms of the compounds. In contrast to the UNIFAC-based and ASOG models, the COSMO-RS model calculates the thermodynamic data first from the molecular surface polarity distributions, which result from quantum chemical calculations of the individual compounds of the mixture. Then, the different interactions of molecules in a liquid, that is, electrostatic interactions, hydrogen bonding, and dispersion, are represented as functions of the surface polarities of the partners. Using an efficient thermodynamic solution for such pairwise surface interactions, COSMO-RS converts the molecular polarity information into standard thermodynamic data.

Computational Details. The details on the model equations, model parameters, and COSMO quantum chemical calculations have been described in previous publications.[70–75] For computational convenience, there are two commercial software packages available for general chemical engineers to use, that is, the ADF (Amsterdam Density Functional) and COSMOtherm programs in which the COSMO-RS model is embedded. It should be mentioned that for a given system, the predicted results coming from the software may differ significantly because some important adjustable parameters (e.g., the interaction parameter α', the effective contact area between two surface segments a_{eff}, the hydrogen-bonding coefficient c_{hb}, and the cut-off surface charge density σ_{hb}) related to the individual atoms are different.[76]

In most cases, an IL molecule is treated as an electroneutral mixture consisting of a cation and an anion. The conformations

of the distinct ions are optimized, and the corresponding COSMO files are stored in the database separately, thus allowing for IL screening from the numerous combinations of cations and anions. Here, we address the issues of how to calculate the activity coefficients at infinite dilution and at finite concentration for binary and ternary systems containing ILs, which are important thermodynamic properties with respect to extractive distillation with ILs.

For a 1:1 IL (i.e., $[A]^+[B]^-$), the activity coefficient at a finite concentration of solute i in the binary mixture (IL + solute) can be calculated by

$$\gamma_i^{\text{bin}} = \frac{\gamma_i^{\text{tern}} \cdot x_i^{\text{tern}}}{x_i^{\text{bin}}} = \frac{\gamma_i^{\text{tern}}}{1+x_{\text{IL}}^{\text{bin}}} \tag{11}$$

where the superscript "tern" represents the hypothetical ternary system comprising cation, anion and solute i, with $x_{\text{cation}}^{\text{tern}} = x_{\text{anion}}^{\text{tern}}$ and $x_{\text{cation}}^{\text{tern}} + x_{\text{anion}}^{\text{tern}} + x_i^{\text{tern}} = 1$; the superscript "bin" represents the binary mixture comprising solute and IL, with $x_{\text{IL}}^{\text{bin}} + x_i^{\text{bin}} = 1$. Thus, according to Eq. 11, the activity coefficient of a solute i in the binary mixture (IL + solute) at infinite dilution is simplified as

$$\gamma_i^{\text{bin}} = 0.5\gamma_i^{\text{tern}} \tag{12}$$

Similarly, for a ternary system comprising component i, component j and IL, the activity coefficient at finite concentration of component i can be calculated by

$$\gamma_i^{\text{tern}} = \frac{\gamma_i^{\text{quart}}}{1+x_{\text{IL}}^{\text{tern}}} \tag{13}$$

where the superscript "quart" represents the hypothetical quaternary system which comprises of cation, anion, solute i, and solute j, with $x_{\text{cation}}^{\text{quart}} = x_{\text{anion}}^{\text{quart}}$; the superscript "tern" represents the ternary system comprising solute i, j, and IL, with $x_{\text{IL}}^{\text{bin}} + x_i^{\text{bin}} + x_j^{\text{bin}} = 1$.

Therefore, care should be taken in the COSMO-RS calculation whenever dealing with the mole fraction transformation. Undoubtedly, the COSMO-RS model is a very efficient predictive tool for screening potential ILs for extractive distillation and other special separation processes.

GCLF EOS

The GCLF EOS is established based on the statistical thermodynamics and can be written as

$$\tilde{P}\tilde{T} = \ln\left(\frac{\tilde{v}}{\tilde{v}-1}\right) + \frac{z}{2}\ln\left(\frac{\tilde{v}+q/r-1}{\tilde{v}}\right) - \theta^2\tilde{T} \tag{14}$$

where $\tilde{P}$, $\tilde{T}$, and $\tilde{v}$ are the reduced pressure, temperature, and molar volume, respectively. The details of the model equations can be found in previous publications.[39,40,77–80] This equation of state contains the following model parameters: group interaction energy ($e_{0,k}$, $e_{1,k}$, $e_{2,k}$), reference volume ($R_{0,k}$, $R_{1,k}$, $R_{2,k}$), and the group binary interaction parameter α_{mn} ($\alpha_{mn}=\alpha_{nm}$). We first extended the predictive GCLF EOS from the systems containing conventional solvents or polymers to systems with ILs[39] and systems of CO_2 and IL.[40]

Equations of state are preferred over activity coefficients for the description of phase equilibria because they can disclose the P (pressure)–V (volume)–T (temperature) relation of the mixture. The density (or volume expansivity) of the mixture of IL and solute is an important physical quantity for the calculation of the liquid volume flow rate along the column internals (e.g., column tray and structured packings) to avoid liquid flooding and ensure that the EDC operates within the feasible operating region.

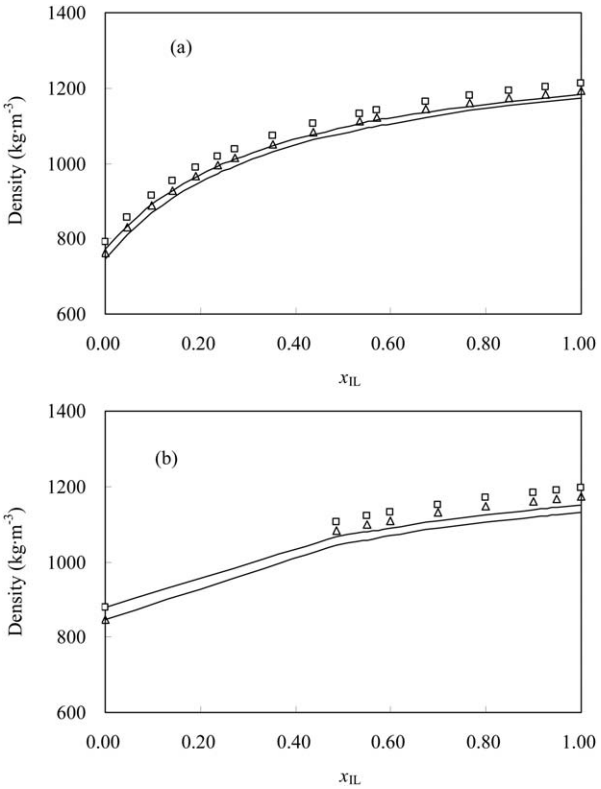

Figure 1. Densities of the mixtures of $[BMIM]^+[MeSO_4]^-$ (1) + ethanol (2) (a) and $[BMIM]^+[BF_4]^-$ (1) + benzene (2) (b) vs. the mole fraction of ILs (x_{IL}) at various temperatures and ambient pressure (1 bar).

(□) $T = 293.15$ K, Ref. 67; (△) $T = 323.15$ K, Ref. 82. Solid lines represent the predicted results by GCLF EOS.

Figure 1 shows the predicted densities of the mixtures of $[BMIM]^+[MeSO_4]^-$ (1) + ethanol (2) and $[BMIM]^+[BF_4]^-$ (1) + benzene (2) at 293.15 K and 323.15 K by GCLF EOS, along with the experimental data.[81,82] It is clear that both the predicted and experimental results agree very well, exhibiting a similar trend that is not exactly based on the mole fraction average of the pure component densities in the usual way. This result is also obvious for other systems. Therefore, in comparison with the predictive activity coefficient models, GCLF EOS is especially suitable for predicting the volumetric properties of systems containing ILs.

Comparison among different predictive thermodynamic models

The activity coefficients at infinite dilution of *n*-alkanes in $[OMIM]^+[Tf_2N]^-$ and *n*-alkanes in $[HMIM]^+[TfO]^-$ are exemplified for the comparison among the original UNIFAC, modified UNIFAC, and COSMO-RS models, as shown in Figure 2. It is evident that the modified UNIFAC model gives the best prediction,[51,52] the original UNIFAC model gives a moderate prediction, and the COSMO-RS model gives the worst prediction. This result is not unusual because the modified UNIFAC model has the most model parameters, whereas the COSMO-RS model is an *a priori* predictive

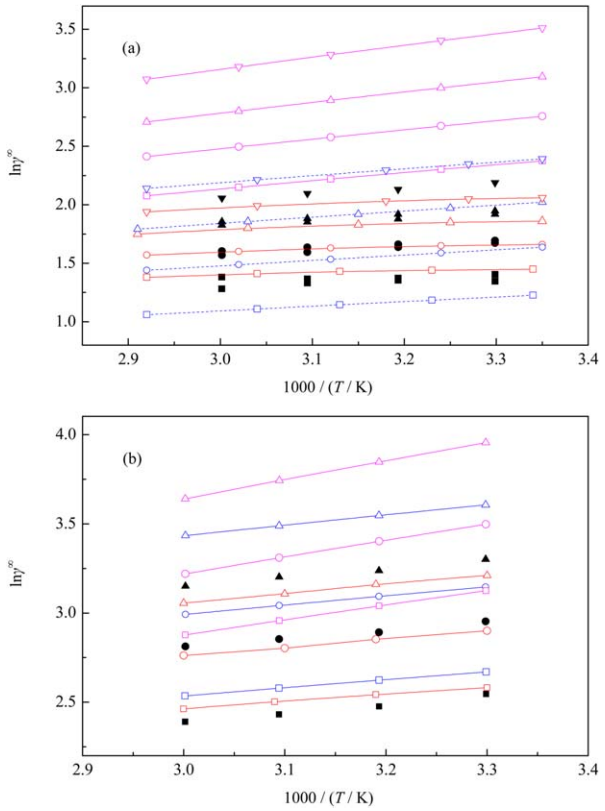

Figure 2. Activity coefficients at infinite dilution of *n*-alkenes in $[OMIM]^+[Tf_2N]^-$ (a) and $[HMIM]^+[TfO]^-$ (b) at a temperature range from 303 to 333 K.

(a) Scattered solid points, experimental data from Ref. 51: (■) pentane; (•) hexane; (▲) heptane; (▼) octane; and (b) Scattered solid points, experimental data from Ref. 52: (■) hexane; (•) heptane; (▲) octane. The empty points with red, blue, and magenta represent the predicted results by the modified UNIFAC, original UNIFAC, and COSMO-RS (ADF version) models, respectively.[Color figure can be viewed in the online issue, which is available at wileyonlinelibrary.com.]

model, independent of the experimental data. However, the actual extractive distillation processes take place in mixtures at finite concentration with the binary and ternary VLE corresponding to the thermodynamic states of the IL recovery separator (e.g., flash drum in vacuum) for the separation of one key component and IL, and of the IL EDC for the separation of two key components using the IL as an entrainer, respectively. The binary P (pressure)–x (mole fraction of solute in the liquid phase) curves of acetone (1) + $[BMIM]^+[Tf_2N]^-$ (2) and benzene (1) + $[MMIM]^+[Tf_2N]^-$ (2) are shown in Figure 3, where it is assumed that no IL appears in the vapor phase due to nonvolatility. As expected, the predicted results by the original UNIFAC model are in better agreement with the experimental data[83,84] than those predicted by the COSMO-RS model. A similar conclusion can be obtained for other systems.

For the isobaric VLE of ternary systems containing ILs, a peculiar experimental phenomenon often occurs. As shown in Figure 4, x_1' and y_1 represent the mole fractions of the light components in the liquid and vapor phases on an IL-free basis, respectively.[85,86] It can be seen that in the isopropanol (or ethanol)-rich region, the lower the IL concentration kept in the liquid phase, the higher is the mole fraction of the light component (e.g., isopropanol or ethanol) in the vapor phase. That is, the addition of IL does not increase the relative volatility of the two components to be separated as expected. This inverse effect is seldom found when using liquid solvents or solid salts as entrainers. More specially, the original UNIFAC model can predict the counterintuitive experimental phenomenon, whereas the COSMO-RS model cannot.

The evidence from the VLE and LLE experiments shows that the COSMO-RS model, although based on the individual atom properties and irrespective of any experimental data, can only reflect the qualitative trend concerning the influence of molecular structures of ILs on the thermodynamic properties, such as the activity coefficients, LLE, and VLE.[87–91] In this regard, we can make full use of the predictive potential of the COSMO-RS model for the CAMD of ILs in extractive distillation and determine the optimal ILs that may not have been synthesized in the laboratory for a specific separation task. In addition, recent studies revealed that the COSMO-RS model is able to estimate the strength of the interactions between solute and IL,[92,93] which is useful for interpreting the underlying separation mechanism as described below.

In summary, the predicted results of thermodynamic properties by the UNIFAC-based models are more accurate than those by the COSMO-RS model. Thus, it is better to use the UNIFAC-based models to establish the equilibrium stage and nonequilibrium stage mathematical models for extractive distillation process simulation and optimization. Meanwhile, for the design of column internals, it is suggested to use the

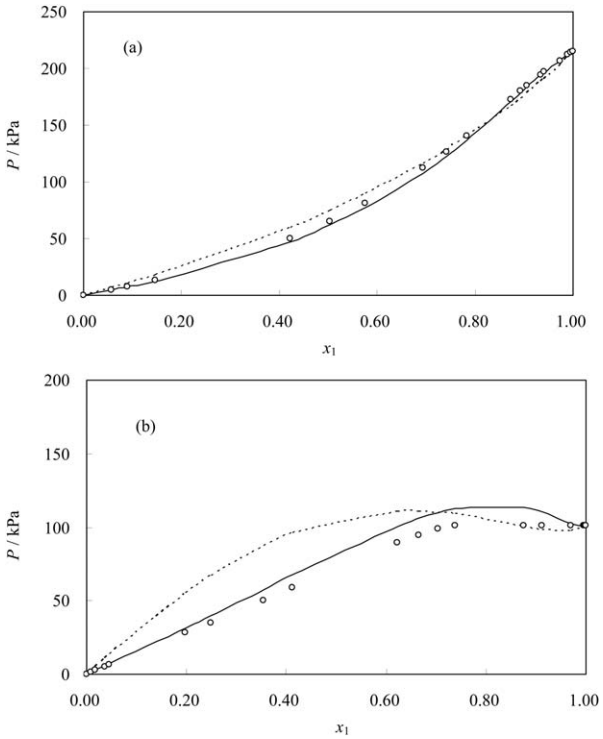

Figure 3. VLE diagrams of acetone (1) + $[BMIM]^+[Tf_2N]^-$ (2) (a) and benzene (1) + $[MMIM]^+[Tf_2N]^-$ (2) (b) at T = 353.15 K.

The solid and dotted lines represent the predicted results by the original UNIFAC model and the COSMO-RS model, respectively.

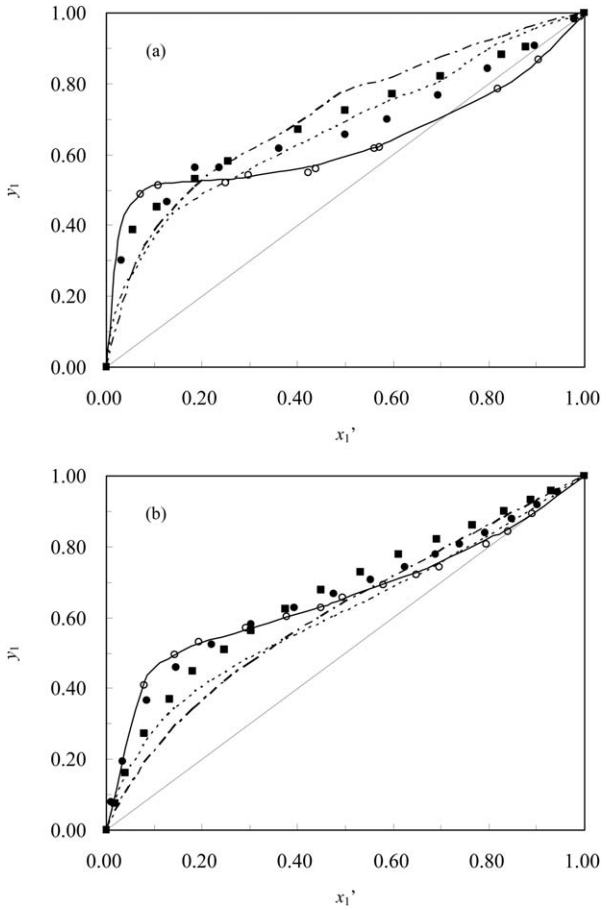

Figure 4. Isobaric VLE diagrams of isopropanol (1) + water (2) + [EMIM]$^+$[BF$_4$]$^-$ (3) (a) and ethanol (1) + water (2) + [EMIM]$^+$[TfO]$^-$ (3) (b) at several IL concentrations.

(a) (○) $x_3 = 0$ (exp.); (•) $x_3 \approx 0.10$ (exp.); (■) $x_3 \approx 0.20$ (exp.); and (b) (○) $x_3 = 0$ (exp.); (•) $x_3 \approx 0.054$ (exp.); (■) $x_3 \approx 0.215$ (exp.). The solid line, dotted line, and dot dashed line represent the predicted results by the original UNIFAC model at $x_3 = 0$, 0.10, and 0.20, respectively.

GCLF EOS to predict the volumetric properties. Therefore, these predictive thermodynamic models complement each other, jointly constructing the chemical engineering fundamentals of extractive distillation with ILs.

Structure-Property Relations

One of the most important scientific issues with respect to extractive distillation with ILs is to identify the relationship between the molecular structures of ILs and the separation performance (namely the structure-property relations) by the combination of predictive thermodynamic models and experiments. However, the structure-property relations are distinct for nonpolar-nonpolar, polar-polar, and nonpolar-nonpolar systems.

Separation of nonpolar-nonpolar systems

The separation of nonpolar-nonpolar systems, such as alkanes/alkenes or aliphatics/aromatics mixtures, is commonly encountered in the petrochemical and chemical industries. Herein, the system of *n*-hexane/1-hexene is taken as a representative of nonpolar/nonpolar systems. It is difficult and expensive to separate them by ordinary distillation because they have close-boiling points. However, extractive distillation with ILs as entrainers is simple and effective for these separations, coupling the advantages of solvent extraction (high separation ability) and distillation (easy operation).

The selectivity and solvent capacity at infinite dilution provide direct evaluation of various ILs for a given separation task. Fortunately, the experimental data on activity coefficients at infinite dilution of solutes in ILs have been extensively measured in recent years. Thus, the selectivity and capacity at infinite dilution for the *n*-hexane (1)/1-hexene (2) separation can be calculated according to Eqs. 1 and 2. Figure 5 shows the predicted results of the selectivity and solvent capacity by the UNIFAC model and the experimental data collected from literature[51,52,70,94–124] at infinite dilution for the separation of *n*-hexane (1) and 1-hexene (2) with ILs. As a whole, the results predicted by the UNIFAC model and the experimental data agree well, and there is a clear compromise between selectivity and solvent capacity. That is, the ILs with a high selectivity at infinite dilution usually have a low solvent capacity. Moreover, the molecular structures of ILs with small molecular volume, unbranched groups and steric shielding effects around the anion charge center (e.g., $[BF_4]^-$, $[Tf_2N]^-$, and $[N(CN)_2]^-$) are favorable for increasing the selectivity and decreasing the capacity. This conclusion was consistent with the previous findings.[125,126] In addition, structure factors, such as hydroxylation and cyaniding on the cation, as well as strong polar group substitution (e.g., alkoxyl group), fluorination, and the inclusion of metal ions on the anion, are favorable for increasing the selectivity of *n*-hexane to 1-hexene at infinite dilution, but they are unfavorable for increasing the solvent capacity. In addition, some ILs, for example, $[DMIM]^+$ $[TCB]^-$, have the higher selectivity and capacity than the benchmark solvent NMP (*N*-methyl-2-pyrrolidone), indicating that ILs may be considered as potential replacements of the traditional volatile organic compounds in extractive distillation.

Recently, more and more ILs have been synthesized and tested as entrainers individually by many researchers. Thus, new structure-property relations should be summarized from the available database to optimize the separation performance of ILs in extractive distillation. In this review, the influence of structural factors on the separation performance is summarized in Table 1, where the symbols "+," "−," and "≈" represent a positive effect, negative effect, and almost no effect, respectively. This enables chemical engineers to quickly assess various combinations of cations and anions in the preselection stage of ILs.

It should be mentioned that the actual operation of the extractive distillation process is conducted at finite concentration, and the conclusions obtained at infinite dilution cannot be directly extrapolated to finite concentration for the separation of nonpolar-nonpolar systems with ILs. However, studies on the ternary VLE of nonpolar-nonpolar systems with ILs are scarce, although they are necessary for understanding the interactions of ILs with the components to be separated in the real state. Liquid-liquid phase demixing may occur according to the rule-of-thumb of "like dissolves like." Mokrushin et al.[127] investigated the separation of propene and propane with several ILs in the miscible region at ambient temperature and low pressure, and found that $[EMIM]^+$ $[B(CN)_4]^-$ is the optimum IL because the introduction of

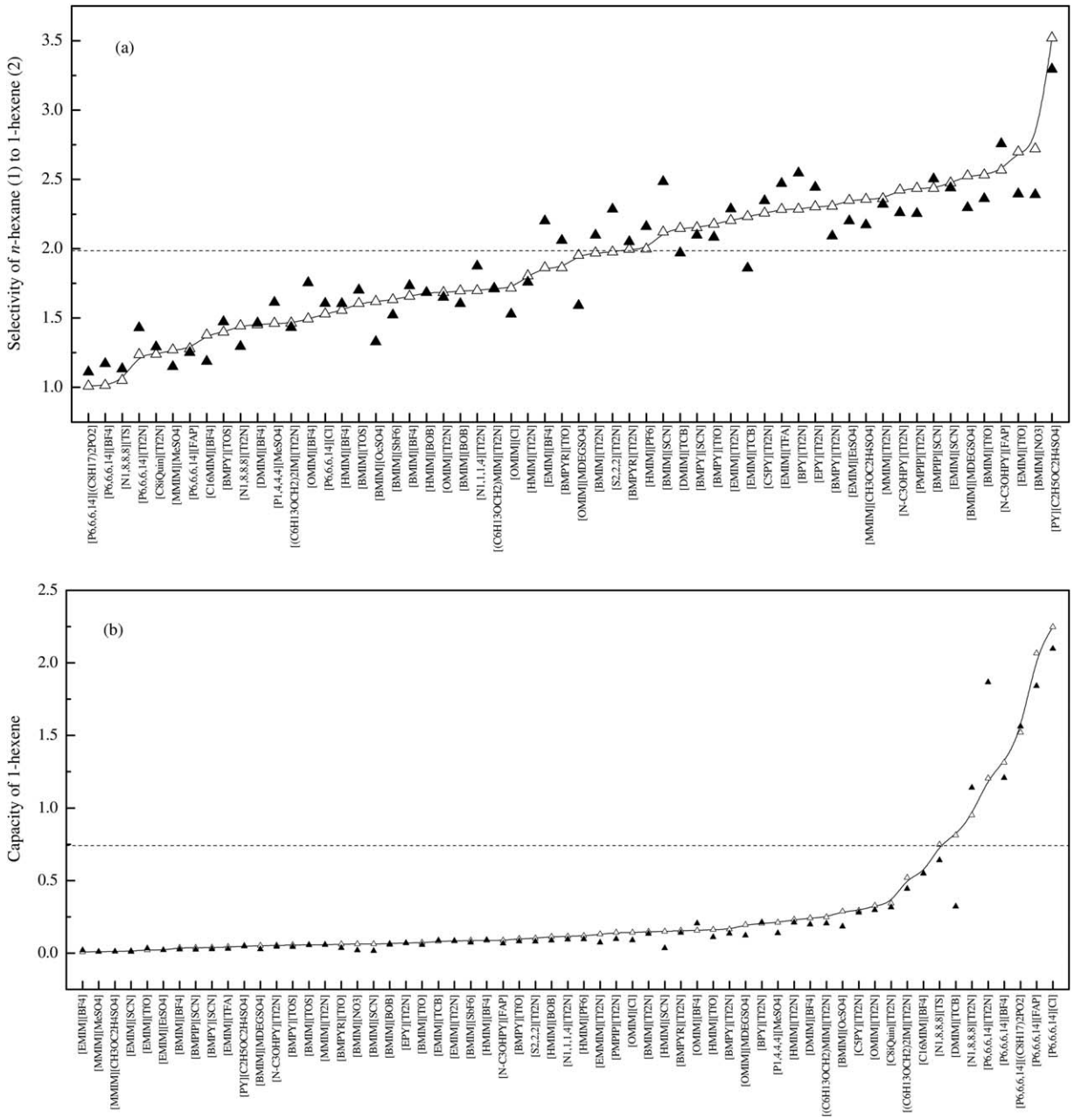

Figure 5. Selectivity of *n*-hexane to 1-hexene and capacity of 1-hexene at infinite dilution for ILs at $T = 298.15$ K.

(a) Selectivity, (b) Capacity. (▲) experimental data from the literature; (△) predicted results by the UNIFAC model; dashed line, NMP.

Table 1. Structure-Property Relations at Infinite Dilution

	Nonpolar-Nonpolar Systems		Polar-Polar Systems		Polar-Nonpolar Systems	
Structural Factors	Selectivity	Solvent Capacity	Selectivity	Solvent Capacity	Selectivity	Solvent Capacity
Short alkyl chain length	+	−	+	+	+	+
Unbranched group	+	−	+	+	+	+
Sterical shielding effect around anion charge center	+	−	−	−	−	−
Cation types (imidazolium, pyrrolidinium, pyridinium-based)	≈	≈	≈	≈	≈	≈
Hydroxylation on the cation	+	−	+	+	+	+
Cyaniding on the cation	+	−	+	≈	+	≈
Alkoxyl substitutions on the anion	+	−	−	−	−	−
Benzyl substitutions on the anion	+	−	−	−	−	−
Fluorination on the anion	+	−	−	−	−	−
Inclusion of metal ions on the anion	+	−	−	−	−	−

CN functional groups into the anion increases the selectivity of propane to propene significantly and at the same time decreases the capacity slightly. This conclusion is consistent with the structure-property relations as listed in Table 1. Unfortunately, the demixing effect was not considered by the authors, and it may take place at high (propene + propane) concentration corresponding to high pressure. Jongmans et al.[128] conducted LLE and LLE experiments for the separation of ethylbenzene and styrene with several ILs and demonstrated that such structural factors as the anion with localized charge (i.e., steric shielding effect) and short alkyl chain length on both cation and anion (i.e., small molecular volume and unbranched group) led to an increase of the ethylbenzene to styrene selectivity but decreased the solvent capacity. The authors measured only a few experimental data on the VLE, and the influence of liquid-liquid phase demixing on the selectivity at finite concentration was not considered in the concentration range investigated because aromatic hydrocarbons usually have a higher solubility in ILs in comparison with other hydrocarbons, such as alkanes and alkenes.

We revealed for the first time that the demixing effect has a significant influence on the selectivity at finite concentration for the separation of 1-hexene and *n*-hexane.[129,130] To achieve a deeper understanding of the effect of the IL concentration on the selectivity, the selectivity of *n*-hexane (1) to 1-hexene (2) with $[BMIM]^+[BF_4]^-$ as the entrainer is presented in Figure 6a, where the left-hand experimental results were obtained in this work at 101.3 kPa and approximately 338 K, as measured by the isobaric VLE technique, and the right-hand experimental data are measured by headspace gas chromatography. The two selectivity curves are almost connected in the vicinity of the dashed line, given that the equilibrium temperature does not fluctuate significantly. The selectivity of *n*-hexane to 1-hexene undergoes an irregular change over the whole concentration range due to phase demixing. As the IL concentration increases, the selectivity of *n*-hexane to 1-hexene initially increases, then decreases after passing through a local extremum, and finally increases again until reaching the maximum selectivity at infinite dilution. Thus, one "selectivity peak" (or separation factor peak) appears over the whole concentration range due to the formation of liquid-liquid phase demixing during the VLE experiments, according to the chemistry rule-of-thumb of "like dissolves like." The LLE diagram for the ternary system is shown in Figure 6b. The formation of a second liquid was observed visually. The IL mainly remained in the lower IL phase and could not exert its effect on the upper organic phase. Thus, liquid-liquid phase demixing is unfavorable for the separation, leading to a decrease in selectivity.

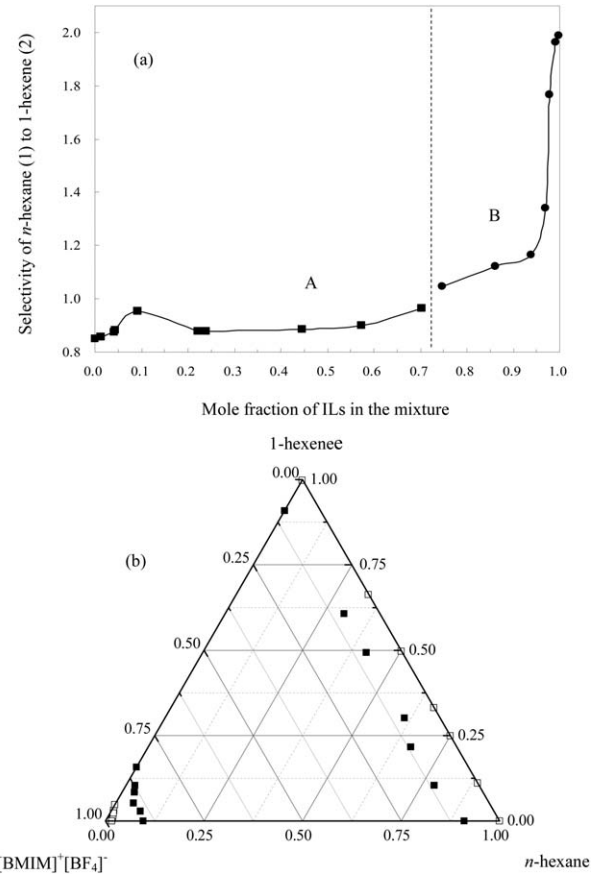

Figure 6. Selectivity of *n*-hexane (1) to 1-hexene (2) at finite concentration using $[BMIM]^+[BF_4]^-$ over the whole concentration range and LLE diagram.

(a) A, experimental data measured by our group; B, experimental data from our previous work.[130] (b) (■), experimental data; (□), COSMO-RS calculations.

Separation of polar-polar systems

The separation of ethanol and water is the most studied system in recent years because anhydrous ethanol is used not only as a chemical reagent and organic solvent but also as the raw material of many important chemical products and intermediates. The dehydration of ethanol can be conducted using several technologies, such as azeotropic distillation, extractive distillation, adsorption, membrane separation, adsorptive distillation, and membrane distillation. Compared with the other techniques, extractive distillation is an energy-efficient technology. In this review, the separation of ethanol and water using extractive distillation with IL was chosen as a model process for the separation of polar-polar systems. Meanwhile, the results derived from this separation may be extended to the separation of other aqueous solutions due to their similar separation mechanisms.

Figure 7 shows the experimental data of the selectivity and capacity at infinite dilution for the ethanol (1)/water (2) separation exhaustively collected from the literature,[115–122,131–141] along with the predicted results by the UNIFAC model. As expected, such structure factors as short alkyl chain length, unbranched group on the IM-based cation, and no steric shielding effect on the anion are favorable for increasing both the selectivity and solvent capacity. In addition, new structure factors, such as hydroxylation and cyaniding on the cation, as well as no substitution groups (e.g., alkyl, benzyl, or alkoxyl group), no fluorination, and no inclusion of metal ion on the anion, are also positive (see Table 1). In this case, there is no need to make a compromise between selectivity and solvent capacity for the selection of suitable ILs for the separation of polar-polar systems. Moreover, the IL $[EMIM]^+[Ac]^-$ is the most promising, possessing the highest selectivity among all of the ILs investigated. We first proposed this potential IL for the separation of ethanol and water,[142] and it was later confirmed by Ge et al.[143] and by Gutierrez et al.[144]

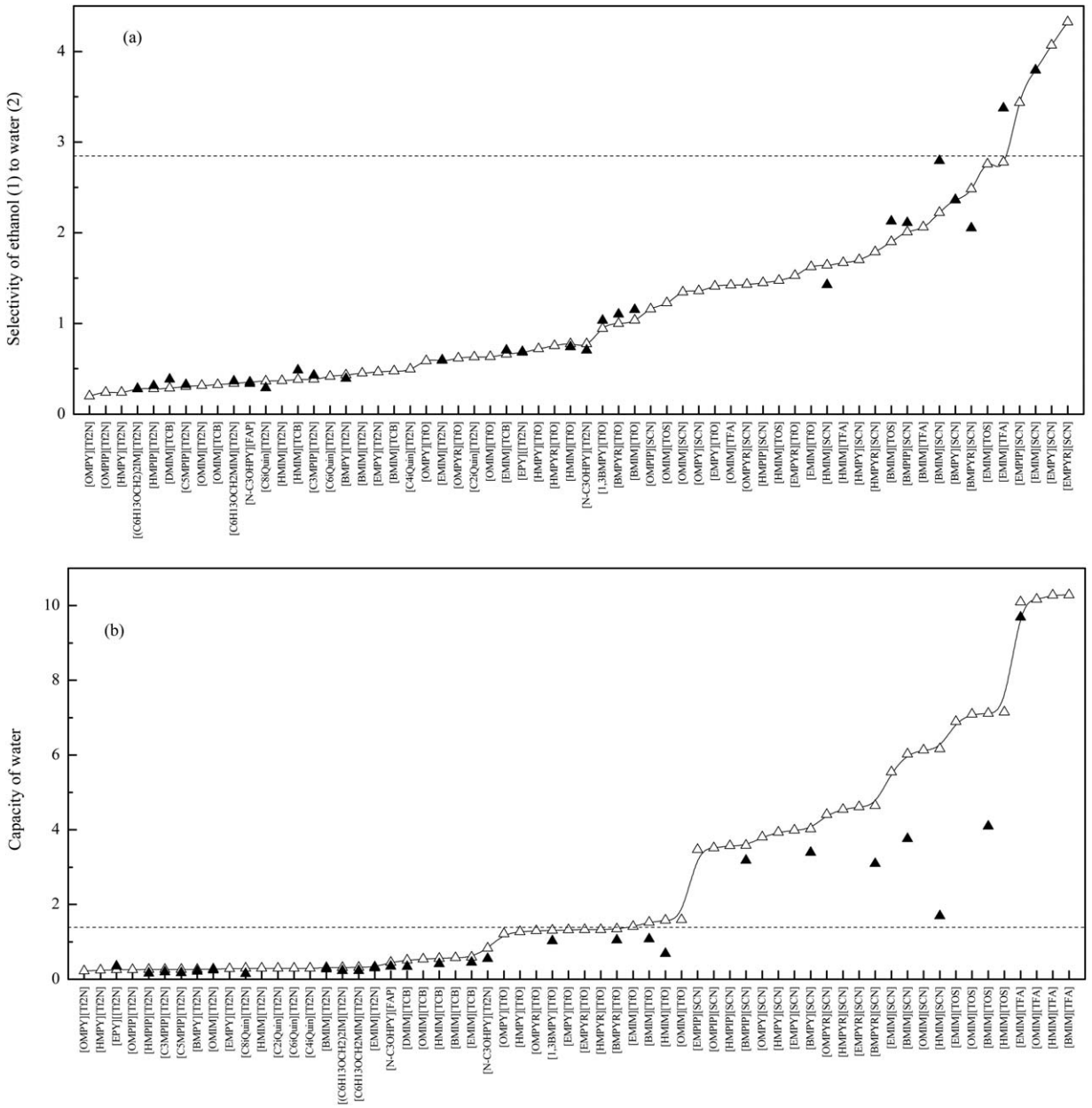

Figure 7. Selectivity of ethanol to water and capacity of water at infinite dilution for various ILs at $T = 298.15$ K.

(a) Selectivity, (b) Capacity. (▲) experimental data from the literature; (△) predicted results by the UNIFAC model; dashed line, EG.

The detailed experimental data of the ternary VLE exhaustively collected from literature by the end of November 2013, which are important for a better understanding of the thermodynamic behavior of such systems and for process simulation and optimization, are provided in Tables S3–S15 in the Supporting Information.[52,85,86,125,126,143–204] Supporting Information Table S16 gives a summarized result. The ternary VLE experimental data available from the literature were mainly measured by research teams from the Beijing University of Chemical Technology (China), Zhejiang University of Technology (China), University of Valencia (Spain), University of Vigo (Spain), Universität Erlangen-Nürnberg (Germany), and Carl von Ossietzky Universität Oldenburg (Germany). However, experimental errors may arise among different data sources. Thus, this urges us to go a further step to compare the separation performance of various ILs for the separation of ethanol (1)/water (2) at the same IL concentration ($x_{IL} = 0.10$) and feeding concentration ($X_1 = 0.90$ and $X_2 = 0.10$ on an IL-free basis). Figure 8 illustrates that the selectivity of ethanol (1) to water (2) follows the order of $[MEA]^+[BF_4]^- > N_{2,2,2,H}]^+[HSO_4]^- > [MMIM]^+[DMPO_4]^- > [BMIM]^+[MeSO_4]^- > [BMIM]^+[Ac]^- \approx [EMPY]^+[EtSO_4]^- > [BMIM]^+[Cl]^- \approx [EMIM]^+[BF_4]^- > [BMIM]^+[BF_4]^- \approx [EMIM]^+[TfO]^- > [HMIM]^+[Cl]^-$, which conforms to the predicted results at infinite state by the UNIFAC model. This demonstrates that these experimental data are reliable to some extent, although they were measured by different research teams.

Separation of polar-nonpolar systems

In principle, extractive distillation with ILs should be suitable for the separation of polar-nonpolar systems (e.g., the mixtures of alcohol + aliphatic hydrocarbons) that form azeotropes. The structure-property relation predicted by the

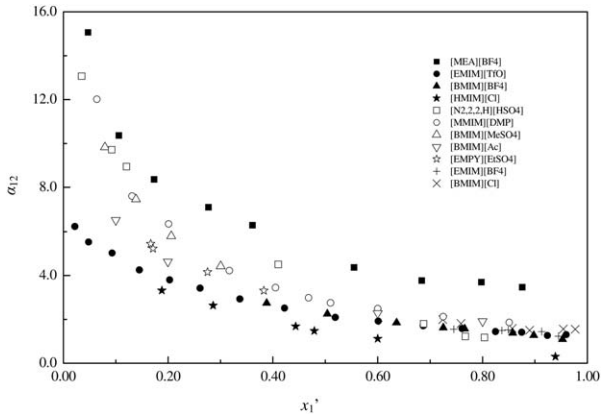

Figure 8. Relative volatility of ethanol (1) to water (2) with ILs as entrainers at $x_3 = 0.10$ at 101.3 kPa.

(■) $[MEA]^+[BF_4]^-$ (Ref. 158); (•) $[EMIM]^+[TfO]^-$ (Ref. 86); (▲) $[BMIM]^+[BF_4]^-$ (Ref. 146); (★) $[HMIM]^+[Cl]^-$ (x_3 in the range from 0.094 to 0.117, Ref. 156); (□) $[N_{2,2,2,H}]^+[HSO_4]^-$ (Ref. 162); (○) $[MMIM]^+$ $[DMPO_4]^-$ (Ref. 159); (△) $[BMIM]^+[MeSO_4]^-$ (x_3 in the range from 0.101 to 0.119, Ref. 150); (▼) $[BMIM]^+[Ac]^-$ (x_3 in the range from 0.095 to 0.120, Ref. 145); (☆) $[EMPY]^+[EtSO_4]^-$ (x_3 in the range from 0.104 to 0.117, Ref. 155); (+) $[EMIM]^+[BF_4]^-$ (Ref. 146); (×) $[BMIM]^+[Cl]^-$ (Ref. 146).

COSMO-RS model at infinite dilution is listed in Table 1, exhibiting a similar trend to the separation of polar-polar systems. However, the ternary VLE experimental data for such systems containing ILs are lacking in the literature; thus, we cannot verify the prediction of the COSMO-RS model at finite concentration.

To break the azeotropic mixtures, another separation method, that is, solvent extraction using ILs as solvents, was also proposed by several researchers.[205–210] It should be noted that solvent extraction (or liquid-liquid extraction) and extractive distillation are two different unit operations in chemical engineering. They are based on different separation mechanisms involving LLE and VLE (or in some cases VLLE), respectively. Thus, the conclusions obtained from LLE cannot be directly extrapolated to VLE, and vice versa. For a simple example, the IL $[EMIM]^+[Ac]^-$ has been proven to be one of the best entrainers for the separation of ethanol and water with extractive distillation. However, it is not a good solvent for the separation of ethanol and water with solvent extraction because $[EMIM]^+[Ac]^-$ is almost miscible with ethanol and water at room temperature. Therefore, the ternary VLE experimental data for the mixtures containing ILs are necessary for better understanding of their thermodynamic behavior and to allow a detailed economic evaluation.

Separation Mechanism

Anion effect

Studies on the separation mechanism have been initiated recently to provide a theoretical insight into the molecular interactions between ILs and the components to be separated. The theory of anion effect speculates that the anion dominates the selectivity (or relative volatility), whereas the cation plays a secondary role, as proposed by Gutierrez et al.[144] However, the conclusion was derived by investigating over a limited number of ILs, where the anion $[Cl]^-$ was kept constant by changing the types of cations. Considering the anion effect, it would be interesting to further investigate the change of selectivity with the carbon number in the alkyl side-chain on the IM-based cations paired with other anions. As shown in Figure 9, as the carbon number in the alkyl side-chain increases, the selectivity tends to decrease first rapidly and then slowly, whether it is the separation for a nonpolar-nonpolar system or for a polar-polar system. That is, when the alkyl side-chain length on the cation is short, both the IL cation and anion have a strong influence on the separation performance of ILs. Therefore, the theory of anion effect may be valid in the case of long alkyl side-chain length on the cation.

Prausnitz and Anderson theory

We first used the theory of Prausnitz and Anderson's solution thermodynamics to clarify the separation mechanism of hydrocarbon mixtures by extractive distillation with ILs as entrainers. In terms of this theory,[211] the selectivity is written as the contributions of three terms, that is, the polar effect P, dispersion effect D, and inductive effect I

$$\mathrm{RT}\ln S_{23} = P + D + I \tag{15}$$

$$P = \delta_{1p}^2 (V_2 - V_3) \tag{16}$$

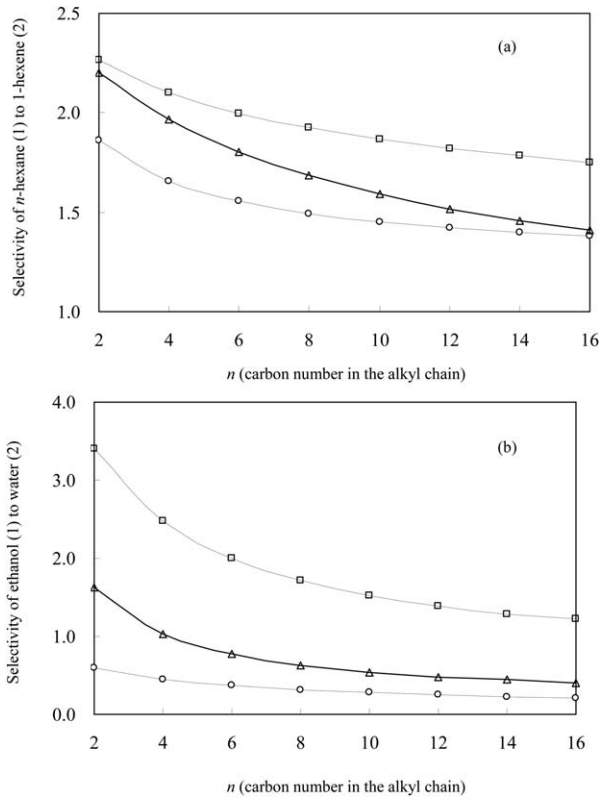

Figure 9. Influence of the carbon number in the alkyl side-chain on the selectivity at infinite dilution for the separations of *n*-hexane/1-hexene (a) and ethanol/water (b) at 298.15 K.

(a) (□) $[R_nMIM]^+[BF_4]^-$; (△) $[R_nMIM]^+[PF_6]^-$; (○) $[R_nMIM]^+[Tf_2N]^-$; and (b) (□) $[R_nMIM]^+[DMP]^-$; (△) $[R_nMIM]^+[TfO]^-$; (○) $[R_nMIM]^+[Tf_2N]^-$. The selectivity at infinite dilution was predicted by the original UNIFAC model.

$$D = V_2(\delta_{1n} - \delta_2)^2 - V_3(\delta_{1n} - \delta_3)^2 \quad (17)$$

$$I = 2V_3\xi_{13} - 2V_2\xi_{12} \quad (18)$$

where the subscripts 1–3 represent IL, the light component and the heavy component to be separated, respectively; V_i is the molar volume of component i; δ_i is the solubility parameter; and ξ_{ij} is the induction energy per unit volume. In general, the polar term P is considerably larger than the sum of D and I. Thus, Eq. 15 becomes

$$\mathrm{RT} \ln S_{23} = \delta_{1p}^2(V_2 - V_3) \approx \delta_1^2(V_2 - V_3) \quad (19)$$

This means that the solubility parameter δ_i can be used to explain the general selectivity trend for a given separation task because the higher solubility parameter is related to the greater selectivity. As we know, the solubility parameter decreases as the alkyl side-chain length on the cation increases. For example, the solubility parameters for the imidazolium-based cations paired with $[Tf_2N]^-$ follow the order of $[EMIM]^+[Tf_2N]^-$ (27.5) > $[BMIM]^+[Tf_2N]^-$ (26.5) > $[HMIM]^+[Tf_2N]^-$ (25.2), where the values in parentheses represent the Hildebrand solubility parameters in the unit of $(J/cm^3)^{1/2}$ coming from the literature.[212,213] The solubility parameters and selectivity exhibit the same order. This also holds for the $[N(n)113]^+[Tf_2N]^-$ series, where both the solubility parameters and selectivity follow the same order of $[N(4)113]^+[Tf_2N]^-$ (26.7) > $[N(6)113]^+[Tf_2N]^-$ (25.8) > $[N(10)113]^+[Tf_2N]^-$ (24.1).

Therefore, this theory provides a correct qualitative analysis for the structure-property relation for the separation of nonpolar-nonpolar systems with ILs, but the disadvantage is such that it is not suitable for the separation of polar-polar systems with ILs because the intermolecular interactions, such as the electrostatic force and hydrogen bonding, are not taken into account.

Process Simulation and Optimization

Process simulation

Single Stage Equilibrium Model. A single stage equilibrium model was established by Chavez-Islas et al.[214] to describe the separation process of ethanol and water with ILs whose molecular structures were optimized by means of a mixed-integer nonlinear programming (MINLP) formulation. The governing equations consist of material balance equations, phase equilibrium equations using the UNIFAC model reported by Lei et al.,[36,37] and mole fraction summation on a single stage at a constant pressure. The optimum IL $[MMIM]^+[DMP]^-$ was finally screened, regardless of the IL recovery from the mixture.

The advantage of the single stage equilibrium model is its fast computation speed, which meets the requirement of CAMD of ILs. However, it is not advisable for rigorous process design for industrial application.

Multistage Equilibrium Model. The rigorous multistage equilibrium model (i.e., equilibrium stage model) was commonly used to simulate the extractive distillation processes with ILs as entrainers using the commercial simulation software. The equations modeling the multistage equilibrium are known as MESH equations. MESH is an acronym referring to the different types of equations. The M equation is the mass balance, E is the phase equilibrium equations, S is the summation equations, and H is the enthalpy balance. A complete extractive distillation process should include an EDC without the entrainer recovery section at the top and an entrainer recovery unit consisting of a flash drum or its combination with another separator, as shown in Figure 10. Note that the high boiling point impurities in the feed should be removed before entering the EDC; otherwise, the impurities accumulated during the operation remain in the entrainer.

The multistage equilibrium model can provide the necessary information for process design, such as the overall heat duty on the condensers and reboilers, as well as the distributions of temperature, composition, liquid and vapor flow rates along the EDC. Seiler et al.[16] used the multistage equilibrium model to simulate the separation of ethanol and water with the IL $[EMIM]^+[BF_4]^-$ and the benchmark solvent EG as entrainers, respectively. In comparison with the conventional extractive distillation process, the overall heat duty with IL as entrainer would save up to 24%. However, they also found that heat integration measures have almost no influence on the reduction of the overall heat duty. On the contrary, Meindersma et al.[31] noted that if no heat integration measure is adopted, the extractive distillation process with IL as entrainer will consume more energy than the conventional process. This may indicate the importance of heat integration when recovering IL from the volatile components. For the separation of ethylbenzene and styrene, the process simulation was performed by Jongmans et al.[215] using the multistage equilibrium model in combination with heat integration. The simulated results showed that the overall energy consumption of the IL $[BMPY]^+[BF_4]^-$ as entrainer was the lowest, in comparison with other investigated ILs and the benchmark solvent sulfolane.

Rate-Based Model. The rate-based model for extractive distillation with ILs was first proposed by Quijada-Maldonado et al.[216] The greatest difference between the equilibrium model and the rate-based model is that the mass and heat transfer rates are considered in every tray or packing segment. Thus, more information on the physical and transport properties of pure components and mixtures should be given or predicted in the rate-based model.[217–220] The process simulation using the rate-based model can be performed by the Aspen Plus software.

It was demonstrated by Quijada-Maldonado et al.[216] that the rate-based model can predict the separation performance of an actual pilot plant for the separation of ethanol and water with $[EMIM]^+[DCA]^-$ as entrainer, with only a 10% deviation from the experimental data. The results showed that for the structured packings, the mass transfer correlations suitable for the conventional solvents can be extrapolated to the systems containing ILs, even at high IL-to-feed ratios.

During the simulation, the physical properties of pure ILs are sometimes not available from the literature, and they have to be estimated by the GCMs.[221–223] In some cases, preliminary experimental work has to be conducted to determine the surface tension, binary diffusion coefficients, and other properties.

Process optimization

For the single EDC, the simultaneous optimization of IL entrainers and the extractive distillation process has been addressed recently by some researchers. To this end, there are two optimization approaches: (1) the molecular structures of ILs were first designed by means of CAMD, and then, the separation scheme was optimized to determine the optimal

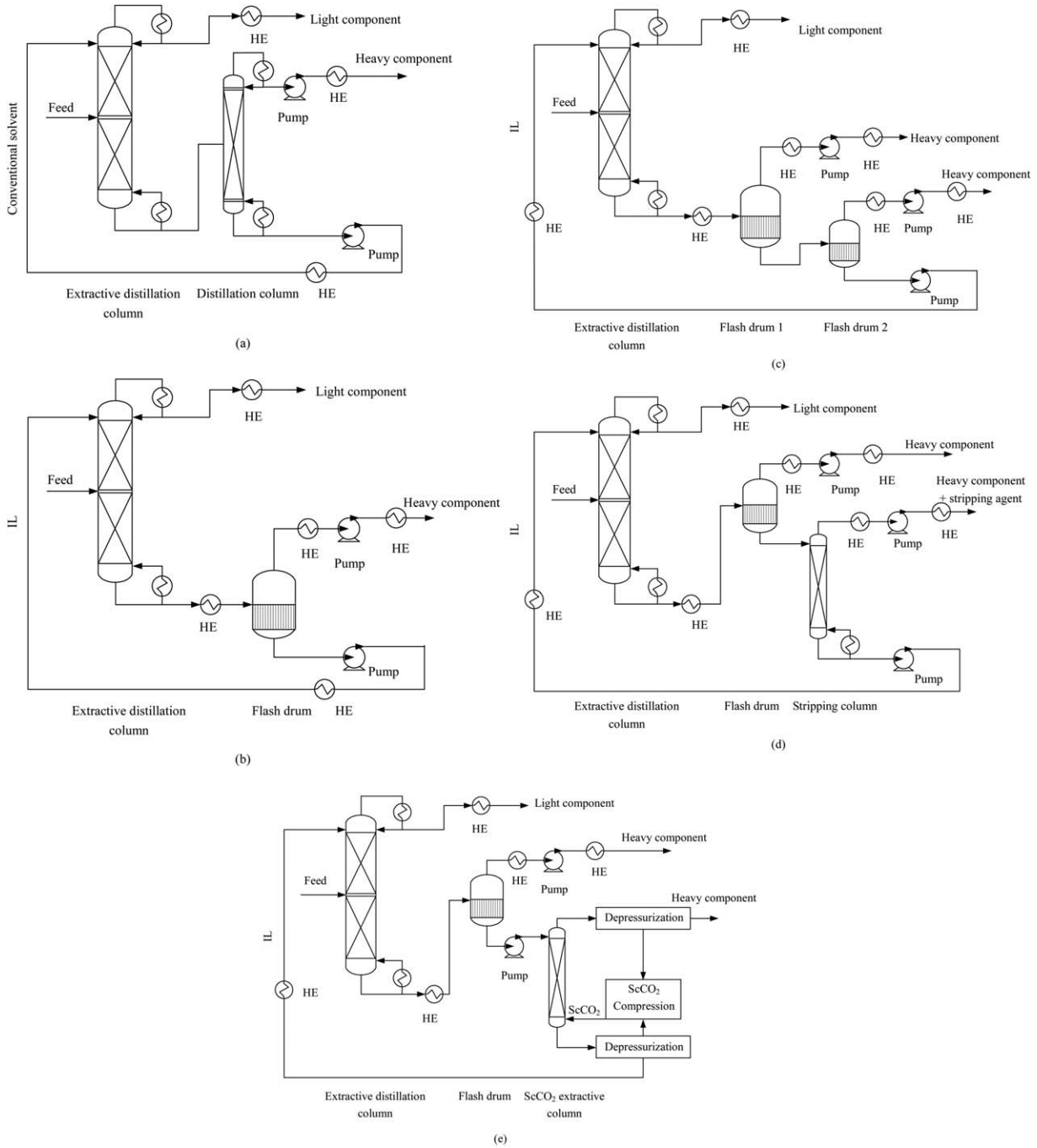

Figure 10. Process schemes for extractive distillation processes with different solvent recovery technologies.

HE stands for heat exchanger. (a) Distillation column for conventional organic solvent recovery. Reproduced from Ref. 31, with permission from American Chemical Society. (b) A flash drum at mild vacuum for IL recovery. Reproduced from Ref. 31, with permission from American Chemical Society. (c) Two flash drums for IL recovery: flash drum 1 at mild vacuum, flash drum 2 at deep vacuum. Reproduced from Ref. 229, with permission from Elsevier. (d) A flash drum at mild vacuum and a stripping column for IL recovery. Reproduced from Ref. 16, with permission from American Institute of Chemical Engineers (AIChE). (e) A flash drum at mild vacuum and a $ScCO_2$ extractive column for IL recovery. Reproduced from Ref. 229, with permission from Elsevier.

design and operating variables using the multistage equilibrium model.[224,225] (2) Both problems were solved in a simultaneous manner in which the MESH equations are incorporated into an MINLP formulation to simulate the EDC, as suggested by Valencia-Marquez et al.[226]

The IL recovery technology is crucial to ensure an economically feasible extractive distillation process. Although it seems that the nonvolatility is always presented as a unique advantage of ILs, this advantage also leads to difficulty in recovering IL with a high purity. For the extractive distillation process using conventional organic solvent, for example, EG, a distillation column is used for the solvent recovery, as shown in Figure 10a. For the extractive distillation process using IL, to recover IL with a high purity, the following three IL recovery technologies are commonly recommended: (1) a flash drum at mild vacuum,[31,227] as shown in Figure 10b; (2) a flash drum at mild vacuum + a flash drum at deep vacuum,[228,229] as shown in Figure 10c; and (3) a flash drum

at mild vacuum + N_2 stripping,[16] as shown in Figure 10d. In the latter two cases, a refrigerant may be required to cool the entrained solutes. Later, Jongmans et al.[229] proposed an additional three technologies for the recovery of styrene from IL: (4) a flash drum at mild vacuum + ethylbenzene stripping, which is similar to the process with a flash drum together with N_2 stripping, as shown in Figure 10d; (5) distillation with the benchmark solvent + IL; and (6) a flash drum at mild vacuum + supercritical CO_2 ($ScCO_2$) extraction, as shown in Figure 10e. A detailed evaluation of the process economics demonstrated that recovery technology numbers 2 and 4 are the best choices.

Comparison among special distillation processes

In this review, we go one step further to compare the energy consumption among extractive distillation, azeotropic distillation, and pressuring swing distillation (PSD). For example, for the separation of ethanol and water, the distillate specification and operating parameters were chosen to be the same as in a previous simulation.[31] It was found that the overall heat duties on condensers and reboilers follow the order of extractive distillation (with $[EMIM]^+[N(CN)_2]^-$ as entrainer) < extractive distillation (with EG as entrainer) < azeotropic distillation (with cyclohexane as entrainer) < PSD (with the combination of P_1 (1 bar) – P_2 (20 bar)) < PSD (with the combination of P_2 (20 bar) – P_1 (1 bar)). This indicates that extractive distillation with ILs is the most advantageous in energy saving. Of course, the present IL $[EMIM]^+[N(CN)_2]^-$ may be further optimized.

Concluding Remarks

This work tries to provide an easy-to-read, comprehensive review for general chemical engineers on extractive distillation with ILs, covering predictive thermodynamic models, structure-property relations, separation mechanisms, and process simulation and optimization. Furthermore, the detailed experimental data of ternary VLE containing ILs, as well as activity coefficients at infinite dilution for organic compounds in ILs, were exhaustively collected in this review. Although much progress has been made in this emerging field, ranging from the molecular level to industrial scale, there are still some scientific issues that remain unsolved. The following points include some of these issues: (1) The VLE experimental data, especially for the ternary systems containing ILs, are still limited, and only a few research groups are taking on this work. This may be attributed to the experimental measurements being tedious and time-consuming. Accordingly, the actual separation performance of many ILs at finite concentration is unknown. (2) For the UNIFAC-based models, many group parameters for ILs are still vacant in the current parameter matrix. Some readers have written to me about the vacancy of group parameters for some interesting ILs. Thus, the UNIFAC-based models should be further developed because the need of general chemical engineers for predictive thermodynamic models is so strong. (3) Engineering studies relevant to column internals (e.g., packings or trays) at high viscosity are lacking. In the design, one should determine whether the conventional pressure drop and mass transfer correlations can be extrapolated to fluids containing ILs and how to improve the separation efficiency of conventional column internals at high viscosity. (4) Finally, all of the studies, thus, far have been limited to the use of single ILs as entrainers. The IL entrainers may be intensified using the mixed ionic liquids or a mixture of ILs and solid inorganic salts, which are easily available from chemical markets, to tune the desirable separation performance, rather than through complicated chemical synthesis of single ILs (e.g., group substitution, fluorination, and inclusion of metal ion).

Although the price of ILs is still higher than many organic solvents, in theory, there is almost no IL loss in the extractive distillation process. Moreover, the price of ILs is currently decreasing. The capital and operational costs of extractive distillation processes with ILs as entrainers should be closely evaluated for future industrial application.

In many extractive distillation processes, the volatile organic solvents will likely be replaced with ILs using the original equipment and only adding one or two flash drums. There is no need to change the main EDC. In view of the potential advantages of extractive distillation with ILs, we are encouraged to continue to perform fundamental research in this promising field because it is a platform technology for the separation of azeotropic or close-boiling mixtures.

Acknowledgment

This work was financially supported by the National Nature Science Foundation of China under Grants (Nos. 21121064 and 21076008).

Literature Cited

1. Lei Z, Chen B, Ding Z. Special Distillation Processes. Amsterdam: Elsevier, 2005.
2. Berg L. Selecting the agent for distillation processes. *Chem Eng Prog*. 1969;65:52–57.
3. Berg L. Separation of benzene and toluene from close boiling nonaromatics by extractive distillation. *AIChE J*. 1983;29:961–966.
4. Momoh SO. Assessing the accuracy of selectivity as a basis for solvent screening in extractive distillation process. *Sep Sci Technol*. 1991;26:729–742.
5. Brennecke JF, Maginn EJ. Ionic liquids: innovative fluids for chemical processing. *AIChE J*. 2001;47:2384–2389.
6. Earle MJ, Esperanca JMSS, Gilea MA, Canongia Lopes JN, Rebelo LPN, Magee JW, Seddon KR, Widegren JA. The distillation and volatility of ionic liquids. *Nature*. 2006;439:831–834.
7. Letcher T. Thermodynamics, Solubility and Environmental Issues. Amsterdam: Elsevier, 2007.
8. Kossack S, Kraemer K, Gani R, Marquardt W. A systematic synthesis framework for extractive distillation processes. *Chem Eng Res Des*. 2008;86:781–792.
9. Hallett JP, Welton T. Room-temperature ionic liquids: solvents for synthesis and catalysis. 2. *Chem Rev*. 2011;111:3508–3576.
10. Lei Z, Li C, Chen B. Extractive distillation: a review. *Sep Purif Rev*. 2003;32:121–213.
11. Lei Z, Wang H, Zhou R, Duan Z. Influence of salt added to solvent on extractive distillation. *Chem Eng J*. 2002;87:149–156.
12. Lei Z, Wang H, Zhou R, Duan Z. Solvent improvement for separating C4 with ACN. *Comput Chem Eng*. 2002;26:1213–1221.
13. Lei Z, Wang H, Zhou R, Duan Z. Process improvement on separating C4 by extractive distillation. *Chem Eng J*. 2002;87:379–386.
14. Beste Y, Eggersmann M, Schoenmakers H. Extractive distillation with ionic liquids. *Chem Ing Technol*. 2005;77:1800–1808.
15. Huang HJ, Ramaswamy S, Tschirner UW, Ramarao BV. A review of separation technologies in current and future biorefineries. *Sep Purif Technol*. 2008;62:1–21.
16. Seiler M, Jork C, Kavarnou A, Arlt W, Hirsch R. Separation of azeotropic mixtures using hyperbranched polymers or ionic liquids. *AIChE J*. 2004;50:2439–2454.
17. Seiler M, Köhler D, Arlt W. Hyperbranched polymers: new selective solvents for extractive distillation and solvent extraction. *Sep Purif Technol*. 2003;30:179–197.
18. Seiler M, Arlt W, Kautz H, Frey H. Experimental data and theoretical considerations on vapor–liquid and liquid–liquid equilibria of

hyperbranched polyglycerol and PVA solutions. *Fluid Phase Equilib.* 2002;201:359–379.
19. Seiler M. Hyperbranched polymers: phase behavior and new applications in the field of chemical engineering. *Fluid Phase Equilib.* 2006;241:155–174.
20. Gorhan A. Production of waterfree ethyl alcohol. US Patent 1,879,847, 1932.
21. Gorhan, A. Apparatus for the manufacture of waterfree ethyl alcohol. US Patent 1,891,593, 1932.
22. Cook RA, Furter WF. Extractive distillation employing a dissolved salt as separating agent. *Can J Chem Eng.* 1968;46:119–123.
23. Llano-Restrepo M, Aguilar-Arias J. Modeling and simulation of saline extractive distillation columns for the production of absolute ethanol. *Comput Chem Eng.* 2003;27:527–549.
24. Hussain MAM, Anthony JL, Pfromm PH. Reducing the energy demand of corn-based fuel ethanol through salt extractive distillation enabled by electrodialysis. *AIChE J.* 2012;58:163–172.
25. Duan Z, Lei L, Zhou R, Ying J, Qian W, Ji S, Jiang W. Study on salt-containing extractive distillation. (I) Preparation of anhydrous alcohol using ethylene glycol and KAc. *Petrochem Technol (China).* 1980;9:350–353.
26. Fu J. Salt-containing model for simulation salt-containing extractive distillation. *AIChE J.* 1996;42:3364–3372.
27. Gil ID, Uyazan AM, Aguilar JL, Rodriguez G, Caicedo LA. Separation of ethonal and water by extractive distillation with salt and solvent as entrainer: process simulation. *Braz J Chem Eng.* 2008; 25:207–215.
28. Arlt M, Seiler M, Jork C, Schneider T. DE Patent 10114734, 2001.
29. Arlt M, Seiler M, Jork C, Schneider T. DE Patent 10136614, 2001.
30. Ionic Liquids in the Dortmund Data Bank. Available at: http://www.ddbst.com/ionic-liquids.html, accessed on June 20, 2014.
31. Meindersma GW, Quijada-Maldonado E, Aelmans TAM, Hernandez JPG, de Haan AB. Ionic liquids in extractive distillation of ethanol/water: from laboratory to pilot plant. In: Visser A, Bridges NJ, Rogers RD, editors. Ionic liquids: Science and Applications. Washington, DC: American Chemical Society, 2012:239–257.
32. Kamihama N, Matsuda H, Kurihara K, Tochigi K, Oba S. Isobaric vapor-liquid equilibria for ethanol + water + ethylene glycol and its constituent three binary systems. *J Chem Eng Data.* 2012;57:339–344.
33. Quijada-Maldonado E, Meindersma GW, de Haan AB. Viscosity and density data for the ternary system water (1)-ethanol (2)-ethylene glycol (3) between 298.15 K and 328.15 K. *J Chem Thermodyn.* 2013;57:500–505.
34. Lei Z, Chen B, Li C, Liu H. Predictive molecular thermodynamic models for liquid solvents, solid salts, polymers, and ionic liquids. *Chem Rev.* 2008;108:1419–1455.
35. Fredenslund A, Jones RL, Prausnitz JM. Group contribution estimation of activity coefficients in nonideal liquid mixtures. *AIChE J.* 1975;21:1086–1099.
36. Bondi A. Van der Waals volumes and radii. *J Phys Chem.* 1964; 68:441–451.
37. Lei Z, Zhang J, Li Q, Chen B. UNIFAC model for ionic liquids. *Ind Eng Chem Res.* 2009;48:2697–2704.
38. Lei Z, Dai C, Liu X, Xiao L, Chen B. Extension of the UNIFAC model for ionic liquids. *Ind Eng Chem Res.* 2012;51:12135–12144.
39. Lei Z, Xiao L, Dai C, Chen B. Group contribution lattice fluid equation of state (GCLF EOS) for ionic liquids. *Chem Eng Sci.* 2012;75:1–13.
40. Lei Z, Dai C, Wang W, Chen B. UNIFAC model for ionic liquid-CO_2 systems. *AIChE J.* 2014;60:716–729.
41. Dai C, Lei Z, Wang W, Xiao L, Chen B. Group contribution lattice fluid equation of state for CO_2–ionic liquid systems: an experimental and modeling study. *AIChE J.* 2013;59:4399–4412.
42. Santiago RS, Santos GR, Aznar M. Liquid-liquid equilibrium in ternary ionic liquid systems by UNIFAC: new volume, surface area and interaction parameters. Part I. *Fluid Phase Equilib.* 2010;295: 93–97.
43. Santiago RS, Aznar M. Liquid-liquid equilibrium in ternary ionic liquid systems by UNIFAC: new volume, surface area and interaction parameters. Part II. *Fluid Phase Equilib.* 2011;303:111–114.
44. Alevizou EI, Pappa GD, Voutsas EC. Prediction of phase equilibrium in mixtures containing ionic liquids using UNIFAC. *Fluid Phase Equilib.* 2009;284:99–105.
45. Gmehling J, Li J, Schiller M. A modified UNIFAC model. 2. Present parameter matrix and results for different thermodynamic properties. *Ind Eng Chem Res.* 1993;32:178–193.
46. Lohmann J, Gmehling J. Modified UNIFAC (Dortmund): reliable model for the development of thermal separation processes. *J Chem Eng Jpn.* 2001;34:43–54.
47. Gmehling J, Lohmann J, Jakob A, Li J, Joh R. A modified UNIFAC (Dortmund) model. 3. Revision and extension. *Ind Eng Chem Res.* 1998;37:4876–4882.
48. Gmehling J, Wittig R, Lohmann J, Joh R. A modified UNIFAC (Dortmund) model. 4. Revision and extension. *Ind Eng Chem Res.* 2002;41:1678–1688.
49. Wittig R, Lohmann J, Gmehling J. Vapor-liquid equilibria by UNIFAC group contribution. 6. Revision and extension. *Ind Eng Chem Res.* 2003, 42:183–188.
50. Nebig S, Bolts R, Gmehling J. Measurement of vapor-liquid equilibria (VLE) and excess enthalpies (H^E) of binary systems with 1-alkyl-3-methylimidazolium bis(trifluoromethylsulfonyl)imide and prediction of these properties and γ^∞ using modified UNIFAC (Dortmund). *Fluid Phase Equilib.* 2007;258:168–178.
51. Kato R, Gmehling J. Systems with ionic liquids: measurement of VLE and γ^∞ data and prediction of their thermodynamic behavior using original UNIFAC, mod. UNIFAC(Do) and COSMO-RS(O1). *J Chem Thermodyn.* 2005;37:603–619.
52. Nebig S, Gmehling J. Measurements of different thermodynamic properties of systems containing ionic liquids and correlation of these properties using modified UNIFAC. *Fluid Phase Equilib.* 2010;294:206–212.
53. Nebig S, Liebert V, Gmehling J. Measurement and prediction of activity coefficients at infinite dilution (γ^∞), vapor-liquid equilibria (VLE) and excess enthalpies (H^E) of binary systems with 1,1-dialkyl-pyrrolidinium bis(trifluoromethylsulfonyl)imide using mod. UNIFAC (Dortmund). *Fluid Phase Equilib.* 2009;277:61–67.
54. Nebig S, Gmehling J. Prediction of phase equilibria and excess properties for systems with ionic liquids using modified UNIFAC: typical results and present status of the modified UNIFAC matrix for ionic liquids. *Fluid Phase Equilib.* 2011;302:220–225.
55. Jakob A, Grensemann H, Lohmann J, Gmehling J. Further development of modified UNIFAC (Dortmund): revision and extension 5. *Ind Eng Chem Res.* 2006;45:7924–7933.
56. Hector T, Gmehling J. Present status of the modified UNIFAC model for the prediction of phase equilibria and excess enthalpies for systems with ionic liquids. *Fluid Phase Equilib.* 2014;371:82–92.
57. Hector T, Uhlig L, Gmehling J. Prediction of different thermodynamic properties for systems of alcohols and sulfate-based anion Ionic Liquids using modified UNIFAC. *Fluid Phase Equilib.* 2013; 338:135–140.
58. Kojima K, Tochigi K. *Prediction of Vapor-Liquid Equilibria by the ASOG Method.* Tokyo: Elsevier, 1979.
59. Tochigi K, Tiegs D, Gmehling J, Kojima K. Determination of new ASOG parameters. *J Chem Eng Jpn.* 1990;23:453–463.
60. Inoue G, Iwai Y, Yasutake M, Honda K, Arai Y. Measurement of infinite dilution dilution activity coefficients of n-alkanes in 4-methyl-n-butylpyridinium tetrafluoroborate using gas-liquid chromatography. *Fluid Phase Equilib.* 2007;251:17–23.
61. Robles PA, Graber TA, Aznar M. Prediction by the ASOG method of liquid-liquid equilibrium for binary and ternary systems containing 1-alkyl-3-methylimidazolium hexafluorophosphate. *Fluid Phase Equilib.* 2009;287:43–49.
62. Robles PA, Graber TA, Aznar M. Prediction of liquid-liquid equilibrium for ternary systems containing ionic liquids with the tetrafluoroborate anion using ASOG. *Fluid Phase Equilib.* 2010;296: 154–158.
63. Klamt A, Jonas V, Burger T, Lohrenz JC. Refinement and parametrization of COSMO-RS. *J Phys Chem A.* 1998;102:5074–5085.
64. Klamt A, Eckert F. COSMO-RS: a novel and efficient method for the a priori prediction of thermophysical data of liquids. *Fluid Phase Equilib.* 2000;172:43–72.
65. Klamt A. Conductor like screening model for real solvents: a new Approach to the quantitative calculation of salvation phenomena. *J Phys Chem.* 1995;99:2224–2235.
66. Diedenhofen M, Klamt A. COSMO-RS as a tool for property prediction of IL mixtures—a review. *Fluid Phase Equilib.* 2010;294: 31–38.
67. Klamet A, Eckert F. Fast solvent screening via quantum chemistry: COSMO-RS approach. *AIChE J.* 2002;48:369–385.
68. Klamt A, Eckert F, Diedenhofen M. Prediction or partition coefficients and activity coefficients of two branched compounds using COSMOtherm. *Fluid Phase Equilib.* 2009;285:15–18.

69. Diedenhofen M, Eckert F, Klamt A. Prediction of infinite dilution activity coefficients of organic compounds in ionic liquids using COSMO-RS. *J Chem Eng Data*. 2003;48:475–479.
70. Banerjee T, Khanna A. Infinite dilution activity coefficients for trihexyltetradecyl phosphonium ionic liquids: measurements and COSMO-RS prediction. *J Chem Eng Data*. 2006;51:2170–2177.
71. Varma NR, Ramalingam A, Banerjee T. Experiments, correlations and COSMO-RS predictions for the extraction of benzothiophene from n-hexane using imidazolium-based ionic liquids. *Chem Eng J*. 2011;166:30–39.
72. Grensemann H, Gmehling J. Performance of a conductor-like screening model for real solvents model in comparison to classical group contribution methods. *Ind Eng Chem Res*. 2005;44:1610–1624.
73. Anantharaj R, Banerjee T. COMS-RS based predictions for the desulphurization of diesel oil using ionic liquids: effect of cation and anion combination. *Fuel Process Technol*. 2011;92:39–52.
74. Banerjee T, Singh MK, Khanna A. Prediction of binary VLE for imidazolium based ionic liquid systems using COSMO-RS. *Ind Eng Chem Res*. 2006;45:3207–3219.
75. Palomar J, Ferro VR, Torrecilla JS, Rodriguez F. Density and molar volume predictions using COSMO-RS for ionic liquids. An approach to solvent design. *Ind Eng Chem Res*. 2007;46:6041–6048.
76. Scientific Computing & Modeling. Available at: http://www.scm.com/Doc/Doc2010/CRS/CRS/page18.html, accessed on June 20, 2014.
77. High MS, Danner RP. Application of the group contribution lattice-fluid EOS to polymer solutions. *AIChE J*. 1990;36:1625–1632.
78. Lee BC, Danner RP. Application of the group-contribution lattice-fluid equation of state to random copolymer-solvent systems. *Fluid Phase Equilib*. 1996;117:33–39.
79. Li J, Lei Z, Chen B, Li C. Extension of the group-contribution lattice-fluid equation of state. *Fluid Phase Equilib*. 2007;260:135–145.
80. Hamedi M, Muralidharan V, Lee BC, Danner RP. Prediction of carbon dioxide solubility in polymers based on a group-contribution equation of state. *Fluid Phase Equilib*. 2003;204:41–53.
81. Iglesias-Otero MA, Troncoso J, Carballo E, Romani L. Densities and excess enthalpies for ionic liquids + ethano or + nitromethane. *J Chem Eng Data*. 2008;53:1298–1301.
82. Hou Y, Xia S, Ma P. Densities of ionic liquids, 1-butyl-3-methylimidazolium hexafluorophosphate and 1-butyl-3-methylimidazolium tetrafluoroborate, with benzene, acetonitrile, and 1-propanol at T = (293.15 to 343.15) K. *J Chem Eng Data*. 2007;52:2077–2082.
83. Kato R, Gmehling J. Measurement and correlation of vapor-liquid equilibria of binary systems containing the ionic liquids [EMIM][$(CF_3SO_2)_2$N], [BMIM][$(CF_3SO_2)_2$N], [MMIM][$(CH_3)_2PO_4$] and oxygenated organic compounds respectively water. *Fluid Phase Equilib*. 2005;231:38–43.
84. Kato R, Krummen M, Gmehling J. Measurement and correlation of vapor-liquid equilibria and excess enthalpies of binary systems containing ionic liquids and hydrocarbons. *Fluid Phase Equilib*. 2004;224:47–54.
85. Li Q, Xing F, Lei Z, Wang B, Chang Q. Isobaric vapor-liquid equilibrium for isopropanol + water + 1-ethyl-3-methylimidazolium tetrafluoroborate. *J Chem Eng Data*. 2008;53:275–279.
86. Orchilles AV, Miguel PJ, Vercher E, Martinez-Andreu A. Using 1-eethyl-3-methylimidazolium trifluoromethanesulfonate as an entrainer for the extractive distillation of ethanol + water mixtures. *J Chem Eng Data*. 2010;55:1669–1674.
87. Ferreira AR, Freire MG, Ribeiro JC, Lopes FM, Crespo JG, Coutinho JAP. An overview of the liquid-liquid equilibria of (ionic liquid + hydrocarbon) binary systems and their modeling by the conductor-like screening model for real solvents. *Ind Eng Chem Res*. 2011;50:5279–5294.
88. Ferreira AR, Freire MG, Ribeiro JC, Lopes FM, Crespo JG, Coutinho JAP. Overview of the liquid-liquid equilibria of ternary systems composed of ionic liquid and aromatic and aliphatic hydrocarbons, and their modeling by COSMO-RS. *Ind Eng Chem Res*. 2012;51:3483–3507.
89. Potdar S, Anantharaj R, Banerjee T. Aromatic extraction using mixed ionic liquids: experiments and COSMO-RS predictions. *J Chem Eng Data*. 2012;57:1026–1035.
90. Banerjee T, Verma KK, Khanna A. Liquid-liquid equilibrium for ionic liquid systems using COSMO-RS: effect of cation and anion dissociation. *AIChE J*. 2008;54:1874–1885.
91. Neves CMSS, Granjo JFO, Freire MG, Robertson A, Oliveira NMC, Coutinho JAP. Separation of ethanol-water mixtures by liquid-liquid extraction using phosphonium-based ionic liquids. *Green Chem*. 2011;13:1517–1526.
92. Gonzalez-Miquel M, Palomar J, Omar S, Rodriguez F. CO_2/N_2 selectivity prediction in supported ionic liquid membranes (SILMs) by COSMO-RS. *Ind Eng Chem Res*. 2011;50:5739–5748.
93. Palomar J, Gonzalez-Miquel M, Polo A, Rodriguez F. Understanding the physical absorption of CO_2 in ionic liquids using the COSMO-RS method. *Ind Eng Chem Res*. 2011;50:3452–3463.
94. Revelli AL, Sprunger LM, Gibbs J, Acree WE, Jr., Baker GA, Mutelet F. Activity coefficients at infinite dilution of organic compounds in trihexyl(tetradecyl)phosphonium bis(trifluoromethylsulfonyl)imide using inverse gas chromatography. *J Chem Eng Data*. 2009;54:977–985.
95. Letcher TM, Reddy P. Determination of activity coefficients at infinite dilution of organic solutes in the ionic liquid, trihexyl(tetradecyl)-phosphonium tris(pentafluoroethyl) trifluorophosphate, by gas–liquid chromatography. *Fluid Phase Equilib*. 2005;235:11–17.
96. Tumba K, Reddy P, Naidoo P, Ramjugernath D. Activity coefficients at infinite dilution of organic solutes in the ionic liquid trihexyl(tetradecyl)phosphonium tetrafluoroborate using gas–liquid chromatography at T = (313.15, 333.15, 353.15, and 373.15) K. *J Chem Thermodyn*. 2011;43:670–676.
97. Reddy P, Gwala NV, Deenadayalu N, Ramjugernath D. Activity coefficients at infinite dilution of organic solutes in the ionic liquid, methyl(trioctyl)ammonium thiosalicylate, [N_{1888}][TS] by gas-liquid chromatography at T = (303.15, 313.15, and 323.15) K. *J Chem Thermodyn*. 2011;43:754–758.
98. Mutelet F, Jaubert JN. Measurement of activity coefficients at infinite dilution in 1-hexadecyl-3-methylimidazolium tetrafluoroborate ionic liquid. *J Chem Thermodyn*. 2007;39:1144–1150.
99. Yan PF, Liu QS, Yang M, Liu XM, Tan ZC, Welz-Biermann U. Activity coefficients at infinite dilution of organic solutes in N-alkylpyridinium bis(trifluoromethylsulfonyl)imide ([C_nPY][NTf_2], n = 2, 4, 5) using gas–liquid chromatography. *J Chem Thermodyn*. 2010;42:1415–1422.
100. Zhang J, Zhang Q, Qiao B, Deng Y. Solubilities of the gaseous and liquid solutes and their thermodynamics of solubilization in the novel room-temperature ionic liquids at infinite dilution by gas chromatography. *J Chem Eng Data*. 2007;52:2277–2283.
101. Foco GM, Bottini SB, Quezada N, de la Fuente JC, Peters C J. Activity coefficients at infinite dilution in 1-alkyl-3-methylimidazolium tetrafluoroborate ionic liquids. *J Chem Eng Data*. 2006;51:1088–1091.
102. Revelli AL, Mutelet F, Turmine M, Solimando R, Jaubert JN. Activity coefficients at infinite dilution of organic compounds in 1-butyl-3-methylimidazolium tetrafluoroborate using inverse gas chromatography. *J Chem Eng Data*. 2009;54:90–101.
103. Foco G, Bermejo MD, Kotlewska A J, van Rantwijk F, Peters CJ, Bottini SB. Activity coefficients at infinite dilution in methylimidazolium nitrate ionic liquids. *J Chem Eng Data*. 2011;56:517–520.
104. Olivier E, Letcher TM, Naidoo P, Ramjugernath D. Activity coefficients at infinite dilution of organic solutes in the ionic liquid 1-butyl-3-methylimidazolium hexafluoroantimonate using gas-liquid chromatography at T = (313.15, 323.15, and 333.15) K. *J Chem Thermodyn*. 2011;43:829–833.
105. David W, Letcher TM, Ramjugernath D, Raal JD. Activity coefficients of hydrocarbon solutes at infinite dilution in the ionic liquid, 1-methyl-3-octyl-imidazolium chloride from gas-liquid chromatography. *J Chem Thermodyn*. 2003;35:1335–1341.
106. Letcher TM, Soko B, Reddy P, Deenadayalu N. Determination of activity coefficients at infinite dilution of solutes in the ionic liquid 1-hexyl-3-methylimidazolium tetrafluoroborate using gas-liquid chromatography at the temperatures 298.15 K and 323.15 K. *J Chem Eng Data*. 2003;48:1587–1590.
107. Heintz A, Casas LM, Nesterov IA, Emel'yanenko VN, Verevkin SP. Thermodynamic properties of mixtures containing ionic liquids. 5. Activity coefficients at infinite dilution of hydrocarbons, alcohols, esters, and aldehydes in 1-methyl-3-butyl-imidazolium bis(trifluoromethyl-sulfonyl) imide using gas-liquid chromatography. *J Chem Eng Data*. 2005;50:1510–1514.
108. Heintz A, Verevkin SP. Thermodynamic properties of mixtures containing ionic liquids. 6. Activity coefficients at infinite dilution of hydrocarbons, alcohols, esters, and aldehydes in 1-methyl-3-octyl-imidazolium tetrafluoroborate using gas-liquid chromatography. *J Chem Eng Data*. 2005;50:1515–1519.

109. Heintz A, Verevkin SP, Ondo D. Thermodynamic properties of mixtures containing ionic liquids. 8. Activity coefficients at infinite dilution of hydrocarbons, alcohols, esters, and aldehydes in 1-hexyl-3-methylimidazolium bis(trifluoromethylsulfonyl) imide using gas-liquid chromatography. *J Chem Eng Data*. 2006;51:434–437.
110. Heintz A, Vasiltsova TV, Safarov J, Bich E, Verevkin SP. Thermodynamic properties of mixtures containing ionic liquids. 9. Activity coefficients at infinite dilution of hydrocarbons, alcohols, esters, and aldehydes in trimethyl-butylammonium bis(trifluoromethylsulfonyl) imide using gas-liquid chromatography and static method. *J Chem Eng Data*. 2006;51:648–655.
111. Heintz A, Kulikov DV, Verevkin, SP. Thermodynamic properties of mixtures containing ionic liquids. 2. Activity coefficients at infinite dilution of hydrocarbons and polar solutes in 1-methyl-3-ethyl-imidazolium bis(trifluoromethyl-sulfonyl) amide and in 1,2-dimethyl-3-ethyl-imidazolium bis(trifluoromethyl-sulfonyl) amide using gas-liquid chromatography. *J Chem Eng Data*. 2002;47:894–899.
112. Domańska U, Paduszynski K. Measurement of activity coefficients at infinite dilution of organic solutes and water in 1-propyl-1-methylpiperidinium bis{(trifluoromethyl)sulfonyl}imide ionic liquid using g.l.c. *J Chem Thermodyn*. 2010;42:1361–1366.
113. Domańska U, Marciniak A. Activity coefficients at infinite dilution measurements for organic solutes and water in the hexyloxymethyl-3-methyl-imidazolium and 1,3-dihexyloxymethyl-imidazolium bis (trifluoromethylsulfonyl)-imide ionic liquids – The cation influence. *Fluid Phase Equilib*. 2009;286:154–161.
114. Domańska U, Marciniak A. Physicochemical properties and activity coefficients at infinite dilution for organic solutes and water in the ionic liquid 1-decyl-3-methylimidazolium tetracyanoborate. *J Phys Chem B*. 2010;114:16542–16547.
115. Domańska U, Zawadzki M, Królikowska M, Tshibangu MM, Ramjugernath D, Letcher TM. Measurements of activity coefficients at infinite dilution of organic compounds and water in isoquinolinium-based ionic liquid [C_8iQuin][NTf_2] using GLC. *J Chem Thermodyn*. 2011;43:499–504.
116. Domańska U, Marciniak A. Activity coefficients at infinite dilution measurements for organic solutes and water in the ionic liquid 4-methyl-N-butyl-pyridinium bis(trifluoromethylsulfonyl)-imide. *J Chem Thermodyn*. 2009;41:1350–1355.
117. Krummen M, Wasserscheid P, Gmehling J. Measurement of activity coefficients at infinite dilution in ionic liquids using the dilutor technique. *J Chem Eng Data*. 2002;47:1411–1417.
118. Kato R, Gmehling J. Activity coefficients at infinite dilution of various solutes in the ionic liquids $[MMIM]^+[CH_3SO_4]^-$, $[MMIM]^+[CH_3OC_2H_4SO_4]^-$, $[MMIM]^+[(CH_3)_2PO_4]^-$, $[C_5H_5NC_2H_5]^+[(CF_3SO_2)_2N]^-$ and $[C_5H_5NH]^+[C_2H_5OC_2H_4OSO_3]^-$. *Fluid Phase Equilib*. 2004;226:37–44.
119. Marciniak A. Activity coefficients at infinite dilution and physicochemical properties for organic solutes and water in the ionic liquid 1-(3-hydroxypropyl)pyridinium bis(trifluoromethylsulfonyl)-amide. *J Chem Thermodyn*. 2011;43:1446–1452.
120. Domańska U, Marciniak A. Activity coefficients at infinite dilution measurements for organic solutes and water in the ionic liquid 1-butyl-3-methylimidazolium trifluoromethanesulfonate. *J Phys Chem B*. 2008;112:11100–111105.
121. Letcher TM, Reddy P. Determination of activity coefficients at infinite dilution of organic solutes in the ionic liquid, trihexyl(tetradecyl)-phosphonium tris(pentafluoroethyl) trifluorophosphate, by gas-liquid chromatography. *Fluid Phase Equilib*. 2005;235:11–17.
122. Domańska U, Królikowska M. Determination of activity coefficients at infinite dilution of 35 solutes in the ionic liquid, 1-butyl-3-methylimidazolium tosylate, using gas-liquid chromatography. *J Chem Eng Data*. 2010;55:4817–4822.
123. Letcher TM, Soko B, Ramjugernath D, Deenadayalu N, Nevines A, Naicker PK. Activity coefficients at infinite dilution of organic solutes in 1-hexyl-3-methylimidazolium hexafluorophosphate from gas-liquid chromatography. *J Chem Eng Data*. 2003;48:708–711.
124. Gwala NV, Deenadayalu N, Tumba K, Ramjugernath D. Activity coefficients at infinite dilution for solutes in the trioctylmethylammonium bis(trifluoromethylsulfonyl)imide ionic liquid using gas-liquid chromatography. *J Chem Thermodyn*. 2010;42:256–261.
125. Jork C, Kristen C, Pieraccini D, Stark A, Chiappe C, Beste YA, Arlt W. Tailor-made ionic liquids. *J Chem Thermodyn*. 2005;37:537–558.
126. Marciniak A. Influence of cation and anion structure of the ionic liquid on extraction processes based on activity coefficients at infinite dilution. A review. *Fluid Phase Equilib*. 2010;294:213–233.
127. Mokrushin V, Assenbaum D, Paape N, Gerhard D, Mokrushina L, Wasserscheid P, Arlt W, Kistenmacher H, Neuendorf S, Goke V. Ionic liquids for propene-propane separation. *Chem Eng Technol*. 2010;33:63–73.
128. Jongmans MTG, Schuur B, de Haan AB. Ionic liquid screening for ethylbenzene/styrene separation by extractive distillation. *Ind Eng Chem Res*. 2011;50:10800–10810.
129. Lei Z, Arlt W, Wasserscheid P. Separation of 1-hexene and n-hexane with ionic liquids. *Fluid Phase Equilib*. 2006;241:290–299.
130. Lei Z, Arlt W, Wasserscheid P. Selection of entrainers in the 1-hexene/n-hexane system with a limited solubility. *Fluid Phase Equilib*. 2007;260:29–35.
131. Paduszyński K, Domańska U. Experimental and theoretical study on infinite dilution activity coefficients of various solutes in piperidinium ionic liquids. *J Chem Thermodyn*. 2013;60:169–178.
132. Marciniak A, Wlazło M. Activity coefficients at infinite dilution measurements for organic solutes and water in the ionic liquid 1-(3-hydroxypropyl)pyridinium trifluorotris(perfluoroethyl)phosphate. *J Phys Chem B*. 2010;114:6990–6994.
133. Domańska U, Lukoshko EV, Wlazło M. Measurements of activity coefficients at infinite dilution for organic solutes and water in the ionic liquid 1-hexyl-3-methylimidazolium tetracyanoborate. *J Chem Thermodyn*. 2012;47:389–396.
134. Domańska U, Królikowska M, Acree WE Jr, Baker GA. Activity coefficients at infinite dilution measurements for organic solutes and water in the ionic liquid 1-ethyl-3-methylimidazolium tetracyanoborate. *J Chem Thermodyn*. 2011;43:1050–1057.
135. Liebert V, Nebig S, Gmehling J. Experimental and predicted phase equilibria and excess properties for systems with ionic liquids. *Fluid Phase Equilib*. 2008;268:14–20.
136. Marciniak A, Wlazlo M. Activity coefficients at infinite dilution measurements for organic solutes and water in the ionic liquid 1-butyl-3-methyl-pyridinium trifluoromethanesulfonate. *J Chem Eng Data*. 2010;55:3208–3211.
137. Domańska U, Marciniak A, Królikowska M, Arasimowicz M. Activity coefficients at infinite dilution measurements for organic solutes and water in the ionic liquid 1-hexyl-3-methylimidazolium thiocyanate. *J Chem Eng Data*. 2010;55:2532–2536.
138. Domańska U, Królikowska M. Measurements of activity coefficients at infinite dilution for organic solutes and water in the Ionic liquid 1-butyl-1-methylpiperidinium thiocyanate. *J Chem Eng Data*. 2011;56:124–129.
139. Domańska U, Laskowska M. Measurements of activity coefficients at infinite dilution of aliphatic and aromatic hydrocarbons, alcohols, thiophene, tetrahydrofuran, MTBE, and water in ionic liquid [BMIM][SCN] using GLC. *J Chem Thermodyn*. 2009;41:645–650.
140. Domańska U, Królikowska M. Measurements of activity coefficients at infinite dilution in solvent mixtures with thiocyanate-based ionic liquids using GLC technique. *J Phys Chem B*. 2010;114:8460–8466.
141. Domańska U, Marciniak A. Activity coefficients at infinite dilution measurements for organic solutes and water in the ionic liquid 1-ethyl-3-methylimidazolium trifluoroacetate. *J Phys Chem B*. 2007;111:11984–11988.
142. Lei Z, Chen B, Li C. COSMO-RS modeling on the extraction of stimulant drugs from urine sample by the double actions of supercritical carbon dioxide and ionic liquid. *Chem Eng Sci*. 2007;62:3940–3950.
143. Ge Y, Zhang L, Yuan X, Geng W, Ji J. Selection of ionic liquids as entrainers for separation of (water + ethanol). *J Chem Thermodyn*. 2008;40:1248–1252.
144. Gutierrez JP, Meindersma GW, de Haan AB. COSMO-RS-based ionic-liquid selection for extractive distillation processes. *Ind Eng Chem Res*. 2012;51:11518–11529.
145. Deng D, Wang R, Zhang L, Ge Y, Ji J. Vapor-liquid equilibrium measurements and modeling for ternary system water + ethanol + 1-butyl-3-methylimidazolium acetate. *Chin J Chem Eng*. 2011;19:703–708.
146. Jork C, Seiler M, Beste YA, Arlt W. Influence of ionic liquids on the phase behavior of aqueous azeotropic systems. *J Chem Eng Data*. 2004;49:852–857.
147. Zhao J, Dong CC, Li CX, Meng H, Wang ZH. Isobaric vapor–liquid equilibria for ethanol–water system containing different ionic liquids at atmospheric pressure. *Fluid Phase Equilib*. 2006;242:147–153.
148. Calvar N, Gonzalez B, Gomez E, Dominguez A. Vapor-liquid equilibria for the ternary system ethanol + water + 1-butyl-3-methylimidazolium

chloride and the corresponding binary systems at 101.3 kPa. *J Chem Eng Data.* 2006;51:2178–2181.
149. Geng W, Zhang L, Deng D, Ge Y, Ji J. Experimental measurement and modeling of vapor–liquid equilibrium for the ternary system water + ethanol + 1-butyl-3-methylimidazolium chloride. *J Chem Eng Data*. 2010;55:1679–1683.
150. Calvar N, González B, Gómez E, DomínguezÁ. Vapor–liquid equilibria for the ternary system ethanol + water + 1-butyl-3-methylimidazolium methylsulfate and the corresponding binary systems at 101.3 kPa. *J Chem Eng Data*. 2009;54:1004–1008.
151. Mokhtarani B, Gmehling J. (Vapour + liquid) equilibria of ternary systems with ionic liquids using headspace gas chromatography. *J Chem Thermodyn*. 2010;42:1036–1038.
152. Li X, Li W, Song X, Ji J. Determination and correlation of the isobaric vapor-liquid equilibrium data for the pseudobinary system of ethanol–water–ionic liquids. *J Zhejiang University Technol*. (in Chinese) 2008;4:399–402.
153. Orchilles AV, Miguel PJ, Flopis FJ, Vercher E, Martinez-Andreu A. Isobaric vapor-liqiuid equilibria for the extractive distillation of ethanol + water mixtures using 1-ethyl-3-methylimidazolium dicyanamide. *J Chem Eng Data*. 2011;56:4875–4880.
154. Calvar N, González B, Gómez E, Domínguez Á. Vapor–liquid equilibria for the ternary system ethanol + water + 1-ethyl-3-methylimidazolium ethylsulfate and the corresponding binary systems containing the ionic liquid at 101.3 kPa. *J Chem Eng Data*. 2008;53:820–825.
155. Calvar N, Gómez E, González B, Domínguez Á. Experimental vapor liquid equilibria for the ternary system ethanol + water + 1-ethyl-3-methylpyridinium ethylsulfate and the corresponding binary systems at 101.3 kPa: study of the effect of the cation. *J Chem Eng Data*. 2010;55:2786–2791.
156. Calvar N, Gonzalez B, Gomez E, Dominguez A. Study of the behaviour of the azeotropic mixture ethanol-water with imidazolium-based ionic liquids. *Fluid Phase Equilib*. 2007;259:51–56.
157. Zhang L, Ge Y, Ji D, Ji J. Experimental measurement and modeling of vapor liquid equilibrium for ternary systems containing ionic liquids: a case study for the system water + ethanol + 1-hexyl-3-methylimidazolium chloride. *J Chem Eng Data*. 2009;54:2322–2329.
158. Liu X, Lei Z, Wang T, Li Q, Zhu J. Isobaric vapor-liquid equilibrium for the ethanol + water + 2-aminoethanol tetrafluoroborate system at 101.3 kPa. *J Chem Eng Data*. 2012;57:3532–3537.
159. Ran X, Wang H, Wang B, Yang X, Zhu W, Li Q. Determination and correlation of vapor-liquid equilibrium for ethanol-water-1,3-dimethylimidazolium dimethylphosphate ternary system. *Petrochem Technol*. (in Chinese) 2011;40:1196–1199.
160. Li Q, Zhu W, Wang H, Ran X, Fu Y, Wang B. Isobaric vapor-liquid equilibrium for the ethanol + water + 1,3-dimethylimidazolium dimethylphosphate system at 101.3 kPa. *J Chem Eng Data*. 2012;57:696–700.
161. Li Q, Wang H, Ran X, Fu Y, Wang B. Vapor-liquid equilibrium and extractive distillation for ethanol-water-ionic liquid ternary system. *Mod Chem Ind*. (in Chinese) 2012;32:69–73.
162. Xin H, Li Q. Isobaric vapor-liquid equilibria for ethanol-water system containing ionic liquids at atmospheric pressure. *CIESC J*. (in Chinese) 2012;63:1678–1683.
163. Orchillés AV, Miguel PJ, Gonzalez-Alfaro V, Vercher E, Martínez-Andreu A. Isobaric vapor–liquid equilibria of 1-propanol + water + trifluoromethanesulfonate-based ionic liquid ternary systems at 100 kPa. *J Chem Eng Data*. 2011;56:4454–4460.
164. Zhang L, Han J, Wang R, Qiu X, Ji J. Isobaric vapor−liquid equilibria for three ternary systems: water + 2-propanol + 1-ethyl-3-methylimidazolium tetrafluoroborate, water + 1-propanol + 1-ethyl-3-methylimidazolium tetrafluoroborate, and water + 1-propanol + 1-butyl-3-methylimidazolium tetrafluoroborate. *J Chem Eng Data*. 2007;52:1401–1407.
165. Zhang L, Guo Y, Deng D, Ge Y. Experimental measurement and modeling of ternary vapor–liquid equilibrium for water + 1-propanol + 1-butyl-3-methylimidazolium chloride. *J Chem Eng Data*. 2013;58:43–47.
166. Matsuda H, Tochigi K, Liebert V, Gmehling J. Vapor–liquid equilibria of ternary systems with 1-ethyl-3-methylimidazolium ethyl sulfate using headspace gas chromatography. *Fluid Phase Equilib*. 2011;307:197–201.
167. Orchillés AV, Miguel PJ, Vercher E, Martínez-Andreu A. Isobaric vapor−liquid equilibria for 1-propanol + water + 1-ethyl-3-methylimidazolium trifluoromethanesulfonate at 100 kPa. *J Chem Eng Data*. 2008;53:2426–2431.
168. Zhang L, Han J, Deng D, Ji J. Selection of ionic liquids as entrainers for separation of water and 2-propanol. *Fluid Phase Equilib*. 2007;255:179–185.
169. Zhang L, Deng D, Han J, Ji D, Ji J. Isobaric vapor−liquid equilibria for water + 2-propanol + 1-butyl-3-methylimidazolium tetrafluoroborate. *J Chem Eng Data*. 2007;52:199–205.
170. Li Q, Zhang J, Lei Z, Zhu J, Wang B, Huang X. Isobaric vapor-liquid equilibrium for (propan-2-ol + water + 1-butyl-3-methylimidazolium tetrafluoroborate). *J Chem Eng Data*. 2009;54:2785–2788.
171. Kim HD, Hwang IC, Park SJ. Isothermal vapor - liquid equilibrium data at T = 333.15 K and excess molar volumes and refractive indices at T = 298.15 K for the dimethyl carbonate + methanol and isopropanol + water with ionic liquids. *J Chem Eng Data*. 2010;55:2474–2481.
172. Döker M, Gmehling J. Measurement and prediction of vapor–liquid equilibria of ternary systems containing ionic liquids. *Fluid Phase Equilib*. 2005;227:255–266.
173. Westerholt A, Liebert V, Gmehling J. Influence of ionic liquids on the separation factor of three standard separation problems. *Fluid Phase Equilib*. 2009;280:56–60.
174. Zhang L, Qiao B, Ge Y, Deng D, Ji J. Effect of ionic liquids on (vapor + liquid) equilibrium behavior of (water + 2-methyl-2-propanol). *J Chem Thermodyn*. 2009;41:138–143.
175. Fang J, Liu J, Li C, Liu Y. Isobaric vapor–liquid equilibrium for the acetonitrile + water system containing different ionic liquids at atmospheric pressure. *J Chem Eng Data*. 2013;58:1483–1489.
176. Orchillés AV, Miguel PJ, Vercher E, Martínez-Andreu A. Isobaric vapor−liquid and liquid−liquid equilibria for chloroform + ethanol + 1-ethyl-3-methylimidazolium trifluoromethanesulfonate at 100 kPa. *J Chem Eng Data*. 2008;53:2642–2648.
177. Orchillés AV, Miguel PJ, Vercher E, Martínez-Andreu A. Isobaric vapor−liquid and liquid−liquid equilibria for chloroform + methanol + 1-ethyl-3-methylimidazolium trifluoromethanesulfonate at 100 kPa. *J Chem Eng Data*. 2010;55:1209–1214.
178. Tian Z, Cui X, Cai J, Zhang Y, Feng T, Peng Y, Xue L. Isobaric VLE data for the system of butan-1-ol + butyl ethanoate + 1-butyl-3-methylimidazolium bis[(trifluoromethyl)sulfonyl]imide. *Fluid Phase Equilib*. 2013;352:75–79.
179. Li R, Cui X, Zhang Y, Feng T, Cai J. Vapor–liquid equilibrium and liquid–liquid equilibrium of ethyl acetate + ethanol + 1-ethyl-3-methylimidazolium acetate. *J Chem Eng Data*. 2012;57:911–917.
180. Li Q, Zhang J, Lei Z, Zhu J, Xing F. Isobaric vapor-liquid equilibrium for ethyl acetate + ethanol + 1-ethyl-3-methylimidazolium tetrafluoroborate. *J Chem Eng Data*. 2009;54:193–197.
181. Li Q, Zhang J, Lei Z, Zhu J, Zhu J, Huang X. Selection of ionic liquids as entrainers for the separation of ethyl acetate and ethanol. *Ind Eng Chem Res*. 2009;48:9006–9012.
182. Orchillés AV, Miguel PJ, Vercher E, Martínez-Andreu A. Isobaric vapor−liquid equilibria for ethyl acetate + ethanol + 1-ethyl-3-methylimidazolium trifluoromethanesulfonate at 100 kPa. *J Chem Eng Data*. 2007;52:2325–2330.
183. Andreatta AE, Francisco M, Rodil E, Soto A, Arce A. Isobaric vapour–liquid equilibria and physical properties for isopropyl acetate + isopropanol + 1-butyl-3-methyl-imidazolium bis(trifluoromethylsulfonyl)imide mixtures. *Fluid Phase Equilib*. 2011;300:162–171.
184. Andreatta AE, Arce A, Rodil E, Soto A. Physical properties and phase equilibria of the system isopropyl acetate + isopropanol + 1-octyl-3-methyl-imidazolium bis(trifluoromethylsulfonyl)imide. *Fluid Phase Equilib*. 2010;287:84–94.
185. Cai F, Wu X, Chen C, Chen X, Asumana C, Haque MR, Yu G. Isobaric vapor–liquid equilibrium for methanol + dimethyl carbonate + phosphoric-based ionic liquids. *Fluid Phase Equilib*. 2013;352:47–53.
186. Chen X, Cai F, Wu X, Asumana C, Yu G. Isobaric vapor–liquid equilibrium for methanol + dimethyl carbonate + 1-butyl-3-methylimidazolium dibutylphosphate. *J Chem Eng Data*. 2013;58:1186–1192.
187. Li Q, Zhu W, Fu Y, Wang H, Li L, Wang B. Isobaric vapor–liquid equilibrium for methanol + dimethyl carbonate + 1-octyl-3-methylimidazolium tetrafluoroborate. *J Chem Eng Data*. 2012;57:1602–1606.
188. Cai J, Cui X, Zhang Y, Li R, Feng T. Isobaric vapor–liquid equilibrium for methanol + methyl acetate + 1-octyl-3-methylimidazolium hexafluorophosphate at 101.3 kPa. *J Chem Eng Data*. 2011;56:2884–2888.
189. Cai J, Cui X, Zhang Y, Li R, Feng T. Vapor-liquid equilibrium and liquid-liquid equilibrium of methyl acetate + methanol + 1-ethyl-3-methylimidazolium acetate. *J Chem Eng Data*. 2011;56:282–287.

190. Orchillés AV, Miguel PJ, Vercher E, Martínez-Andreu A. Isobaric vapor−liquid equilibria for methyl acetate + methanol + 1-ethyl-3-methylimidazolium trifluoromethanesulfonate at 100 kPa. *J Chem Eng Data*. 2007;52:915–920.
191. Hwang IC, Park SJ, Han KJ. Vapor–liquid equilibria at 333.15 K and excess molar volumes and deviations in molar refractivity at 298.15 K for mixtures of diisopropyl ether, ethanol and ionic liquids. *Fluid Phase Equilib*. 2011;309:145–150.
192. Hwang IC, Kwon RH, Park SJ. Azeotrope breaking for the system ethyl tert-butyl ether (ETBE) + ethanol at 313.15 K and excess properties at 298.15 K for mixtures of ETBE and ethanol with phosphonium-based ionic liquids. *Fluid Phase Equilib*. 2013;344:32–37.
193. Mokhtarani B, Valialahi L, Heidar KT, Mortaheb HR, Sharifi A, Mirzaei M. Experimental study on (vapor + liquid) equilibria of ternary systems of hydrocarbons ionic liquid using headspace gas chromatography. *J Chem Thermodyn*. 2012;51:77–81.
194. Mokhtarani B, Valialahi L, Heidar KT, Mortaheb HR, Sharifi A, Mirzaei M. Effect of 1-methyl 3-octylimidazolium thiocyanate on vapor–liquid equilibria of binary mixtures of hydrocarbons. *Fluid Phase Equilib*. 2012;334:65–69.
195. Cehreli S, Gmehling J. Phase equilibria for benzene-cyclohexene and activity coefficients at infinite dilution for the ternary systems with ionic liquids. *Fluid Phase Equilib*. 2010;259:125–129.
196. Jongmans MTG, Hermens E, Schuur B, de Haan AB. Binary and ternary vapor−liquid equilibrium data of the system ethylbenzene + styrene + 3-methyl-N-butylpyridinium tetracyanoborate at vacuum conditions and liquid–liquid equilibrium data of their binary systems. *Fluid Phase Equilib*. 2012;315:99–106.
197. Jongmans MTG, Raijmakers M, Schuur B, de Haan A. Binary and ternary vapor−liquid equilibrium data of the system (ethylbenzene + styrene + 4-methyl-N-butylpyridinium tetrafluoroborate) at vacuum conditions and liquid−liquid equilibrium data of their binary systems. *J Chem Eng Data*. 2012;57:626–633.
198. Li Q, Cao L, Sun X, Liu P, Wang B. Isobaric vapor–liquid equilibrium for ethyl acetate + acetonitrile + 1-butyl-3-methylimidazolium hexafluorophosphate at 101.3 kPa. *J Chem Eng Data*. 2013;58:1112–1116.
199. Li Q, Sun X, Cao L, Wang B, Chen Z, Zhang Y. Effect of ionic liquids on the isobaric vapor–liquid equilibrium behavior of methanol–methyl ethyl ketone. *J Chem Eng Data*. 2013;58:1133–1140.
200. Orchillés AV, Miguel PJ, Llopis FJ, Vercher E, Martínez-Andreu A. Influence of some ionic liquids containing the trifluoromethanesulfonate anion on the vapor–liquid equilibria of the acetone + methanol system. *J Chem Eng Data*. 2011;56:4430–4435.
201. Orchilles AV, Miguel PJ, Gonzalez-Alfaro V, Vercher E, Martinez-Andreu A. 1-Ethyl-3-methylimidazolium dicyanamide as a very efficient entrainer for the extractive distillation for the acetone + methanol system. *J Chem Eng Data*. 2012;57:394–399.
202. Matsuda H, Liebert V, Tochigi K, Gmehling J. Influence of sulfate-based anion ionic liquids on the separation factor of the binary azeotropic system acetone + methanol. *Fluid Phase Equilib*. 2013;340:27–30.
203. Orchilles AV, Miguel PJ, Vercher E, Martinez-Andreu A. Ionic liquids as entrainers in extractive distillation: isobaric vapor-liquid equilibria for acetone + methanol + 1-ethyl-3-methylimidazolium trifluoromethanesulfonate. *J Chem Eng Data*. 2007;52:141–147.
204. Zhu J, Chen J, Li C, Fei W. Study on the separation of 1-hexene and trans-3-hexene using ionic liquids. *Fluid Phase Equilib*. 2006;247:102–106.
205. Pereiro AB, Araujo JMM, Esperanca JMSS, Marrucho IM, Rebelo LPN. Ionic liquids in separations of azeotropic systems—a review. *J Chem Thermodyn*. 2012;46:2–28.
206. Meindersma GW, Hansmeier AR, de Haan AB. Ionic liquids for aromatics extraction. *Present status and future outlook*. *Ind Eng Chem Res*. 2010;49:7530–7540.
207. Domanska U, Zolek-Tryznowska Z, Pobudkowska A. Separation of hexane/ethanol mixtures. LLE of ternary systems (ionic liquid or hyperbranched polymer + ethanol + hexane) at T = 298.15 K. *J Chem Eng Data*. 2009;54:972–976.
208. Arce A, Earle MJ, Rodriguez H, Seddon KR. Separation of aromatic hydrocarbons from alkanes using the ionic liquid 1-ethyl-3-methylimidazolium bis{(trifluoromethyl) sulfonyl}amide. *Green Chem*. 2007;9:70–74.
209. Pereiro AB, Rodriguez A. Separation of ethanol-heptane azeotropic mixtures by solvent extraction with an ionic liquid. *Ind Eng Chem Res*. 2009;48:1579–1585.
210. Revelli AL, Mutelet F, Jaubert JN. Extraction of n-alcohols from n-heptane using ionic liquids. *J Chem Eng Data*. 2011;56:3873–3880.
211. Prausnitz JM, Anderson R. Thermodynamics of solvent selectivity in extractive distillation of hydrocarbons. *AIChE J*. 1961;7:96–101.
212. Kilaru PK, Condemarin RA, Scovazzo P. Correlations of low-pressure carbon dioxide and hydrocarbon solubilities in imidazolium-, phosphonium-, and ammonium-based room-temperature ionic liquids. Part 1. Using surface tension. *Ind Eng Chem Res*. 2008;47:900–909.
213. Kilaru PK, Scovazzo P. Correlations of low-pressure carbon dioxide and hydrocarbon solubilities in imidazolium-, phosphonium-, and ammonium-based room-temperature ionic liquids. Part 2. Using activation energy of viscosity. *Ind Eng Chem Res*. 2008;47:910–919.
214. Chavez-Islas LM, Vasquez-Medrano R, Flores-Tlacuahuac A. Optimal molecular design of ionic liquids for high-purity bioethanol production. *Ind Eng Chem Res*. 2011;50:5153–5168.
215. Jongmans MTG, Hermens E, Raijmakers M, Maassen JIW, Schuur B, de Haan AB. Conceptual process design of extractive distillation processes for ethylbenzene/styrene separation. *Chem Eng Res Des*. 2012;90:2086–2100.
216. Quijada-Maldonado E, Aelmans TAM, Meindersma GW, de Haan AB. Pilot plant validation of a rate-based extractive distillation model for water-ethanol separation with the ionic liquid [emim][DCA] as solvent. *Chem Eng J*. 2013;223:287–297.
217. Taylor R, Krishna R. Modelling reactive distillation. *Chem Eng Sci*. 2000;55:5183–5229.
218. Lei ZG, Li CY, Chen BH, Wang EQ, Zhang JC. Study on the alkylation of benzene and 1-dodecene. *Chem Eng J*. 2003;93:191–200.
219. Krishnamurthy R, Taylor R. A nonequilibrium stage model for multicomponent separation processes part I: model description and method of solution. *AIChE J*. 1985;31:449–456.
220. Krishnamurthy R, Taylor R. A nonequilibrium stage model for multicomponent separation processes Part II: comparison with experiment. *AIChE J*. 1985;31:456–465.
221. Valderrama JO, Rojas RE. Critical properties of ionic liquids. *Revisited*. *Ind Eng Chem Res*. 2009;48:6890–6900.
222. Valderrama JO, Zarricueta K. A simple and generalized model for predicting the density of ionic liquids. *Fluid Phase Equilib*. 2009;275:145–151.
223. Remesh LG, Coutinho JAP. A group contribution method for heat capacity estimation of ionic liquids. *Ind Eng Chem Res*. 2008;47:5751–5757.
224. Chavez-Islas LM, Vasquez-Medrano R, Flores-Tlacuahuac A. Optimal synthesis of a high purity bioethanol distillation column using ionic liquids. *Ind Eng Chem Res*. 2011;50:5175–5190.
225. Roughton BC, Christian B, White J, Camarda KV, Gani R. Simultaneous design of ionic liquid entrainers and energy efficient azeotropic separation processes. *Comput Chem Eng*. 2012;42:248–262.
226. Valencia-Marquez D, Flores-Tlacuahuac A, Vasquez-Medrano R. Simultaneous optimal design of an extractive column and ionic liquid for the separation of bioethanol-water mixtures. *Ind Eng Chem Res*. 2012;51:5866–5880.
227. Li Q, Zhang J, Wang B, Ni J. Process simulation on the separation of ethyl acetate and ethanol by extractive distillation with ionic liquids. *Chem Ind Eng Prog (China)*. 2009;28:288–290.
228. Shiflett MB, Yokozeki A. Separation of difluoromethane and pentafluoroethane by extractive distillation using ionic liquid. *Chem Today*. 2006;24:28–29.
229. Jongmans MTG, Trampe J, Schuur B, de Haan AB. Solute recovery from ionic liquids: a conceptual design study for recovery of styrene monomer from [4-mebupy][BF_4]. *Chem Eng Process*. 2013;70:148–161.

Manuscript received Apr. 19, 2014.